Journal of Nuclear Medicine, published on December 20, 2019 as doi:10.2967/jnumed.119.234922

Radiohybrid ligands: a novel tracer concept exemplified by ^{18}F- or ^{68}Ga-labeled rhPSMA-inhibitors

Alexander Wurzer[1], Daniel Di Carlo[1], Alexander Schmidt[1], Roswitha Beck[1], Matthias Eiber[2], Markus Schwaiger[2] and Hans-Jürgen Wester[1]

[1] Chair of Pharmaceutical Radiochemistry, Technical University of Munich, Garching, Germany;

[2] Department of Nuclear Medicine, Klinikum rechts der Isar, Technical University of Munich, Munich, Germany.

First author:

Alexander Wurzer

Phone: +49.89.289.12203

Fax : +49.89.289.12204

Email: Alexander.Wurzer@tum.de

Corresponding author:

Hans-Jürgen Wester, PhD

Phone: +49.89.289.12203

Fax: +49.89.289.12204

Email: H.J.Wester@tum.de

Address of first author and corresponding author:

Technical University of Munich,

Chair of Pharmaceutical Radiochemistry,

Walther-Meißner-Str. 3

85748 Garching

GERMANY

ABSTRACT

When we critically assess the reason for the current dominance of ^{68}Ga-labeled peptides and peptide-like ligands in radiopharmacy and nuclear medicine we have to conclude that the major advantage of such radiopharmaceuticals is the apparent lack of suitable ^{18}F-labeling technologies with proven clinical relevance. **Aim:** In order to prepare and to subsequently perform a clinical proof-of-concept study on the general suitability of Silicon-Fluoride-Acceptor (SiFA) conjugated radiopharmaceuticals we developed inhibitors of the prostate-specific membrane antigen (PSMA) that are labeled by isotopic exchange (IE). To compensate for the pronounced lipophilicity of the SiFA unit we utilized metal chelates, conjugated in close proximity to SiFA. Six different radiohybrid PSMA ligands (rhPSMA-ligands) were evaluated and compared with the commonly used ^{18}F-PSMA-inhibitors ^{18}F-DCFPyL and ^{18}F-PSMA-1007. **Methods:** All inhibitors were synthesized by solid-phase peptide synthesis. Human serum albumin (HSA) binding was measured by affinity high-performance liquid chromatography, while the lipophilicity of each tracer was determined by the *n*-octanol/buffer method. *In vitro* studies (IC_{50}, internalization) were carried out on LNCaP cells. Biodistribution studies were conducted on LNCaP tumor-bearing male CB-17 SCID mice. **Results:** On the laboratory scale (starting activities: 0.2–9.0 GBq), labeling of ^{18}F-rhPSMA-5 to 10 by IE was completed in <20 min (radiochemical yields: 58 ± 9%, radiochemical purity: >97%) with molar activities of 12–60 GBq/μmol. All rhPSMAs showed low nanomolar affinity and high internalization by PSMA expressing cells when compared with the reference radiopharmaceuticals, medium-to-low lipophilicity and high HSA binding. Biodistribution studies in LNCaP tumor-bearing mice revealed high tumor uptake, sufficiently fast clearance kinetic from blood, low hepatobiliary excretion, fast renal excretion and very low uptake of ^{18}F-activity in bone. **Conclusion:** The novel ^{18}F-rhPSMA radiopharmaceuticals developed under the radiohybrid concept, show equal or better targeting characteristics than the established ^{18}F-PSMA-tracers, ^{18}F-DCFPyL and ^{18}F-PSMA-1007. The unparalleled simplicity of production, the possibility to produce the identical ^{68}Ga-labeled ^{19}F-^{68}Ga-rhPSMA-tracers and the possibility to extend this concept to true theranostic radiohybrid radiopharmaceuticals, such as F-Lu-rhPSMA, are unique features of these radiopharmaceuticals.

Keywords: PSMA, fluorine-18, prostate cancer, radiohybrid

INTRODUCTION

Since the clinical introduction of ^{68}Ga-labeled somatostatin receptor ligands in the first decade of this century, ^{68}Ga has gained increased interest and importance. As a consequence, more and more peptidic radiopharmaceuticals have been developed and assessed whereupon approved ^{68}Ge/^{68}Ga-generators have become commercially available. Thus, fostered by the success of the first ^{68}Ga-radiopharmaceuticals, such as the approved ^{68}Ga-labeling kits NETSPOT (kit for the preparation of ^{68}Ga-DOTATATE) and SOMAKIT TOC (kit for the preparation of ^{68}Ga-DOTATOC), a unique "^{68}Ge/^{68}Ga-generator-based radiopharmacy concept" has been established in parallel to the cyclotron-based production of radiopharmaceuticals (*1,2*). Although "fast and cheap production" and "ease of generator-based syntheses" are widely accepted unique features of this concept, it has to be noted that these assessments are based on a comparison with the current clinically established state-of-the-art ^{18}F-labeling technologies.

When we critically assess the reason for the current relevance of ^{68}Ga in radiopharmacy and nuclear medicine we have to conclude that the apparent lack of suitable ^{18}F-labeling technologies with proven clinical relevance is the major advantage for ^{68}Ga-labeled peptides and peptide-like radiopharmaceuticals.

While ^{68}Ga-labeling by complexation is fast and efficient, none of the current clinically established ^{18}F-labeling technologies can offer comparable levels of simplicity and speed (*3-5*). In order to overcome these limitations, a variety of alternative ^{18}F-labeling techniques have been investigated and assessed, and the range of ^{18}F-labeling has been extended from C-^{18}F bond formation to the formation of ^{18}F-bonds with silicon (*6*), boron (*7*) and aluminum (*8*).

The latter relies on the strong chemical bond between aluminum and fluoride, which is exploited for complexation of ^{18}F-AlF^{2+}, especially by suitable NOTA- (1,4,7-triazacyclononane-1,4,7-triacetic acid-) conjugated ligands (*8,9*). In the recent publication of Liu et al. a new NOTA-derivative of PSMA-617, Al^{18}F-PSMA-BCH, is described (*10*). Its production is carried out in a formal two step-procedure, consisting of the formation of ^{18}F-AlF^{2+} (5 min at ambient temperature (r.t.)) and subsequent complexation by means of 80 nmol precursor at 110 °C for 15 min and purification by a simple solid phase extraction (SPE) process. Manual syntheses yielded the product in 32±5% radiochemical yield (RCY) and 99% radiochemical purity

(RCP) (*10*). Further elegant labeling approaches based on boron compounds were introduced by Perrin and co-workers (*11,12*). Herein, arylfluoroborates were applied for synthesis of PET-probes by means of ^{18}F nucleophilic substitution of borate esters or ^{19}F-^{18}F isotopic exchange (IE) of organotrifluoroborates (*7,11-13*). In a recent paper of Kuo and colleagues on eight different trifluoroborate-conjugated PSMA-inhibitors, the labeling started with about 37 GBq and resulted in 4-16% yield (uncorrected) when using 100 nmol precursor (*12*). To obtain high RCP (>99%), HPLC (high-performance liquid chromatography) purification was necessary; when HPLC purification was replaced by SPE, RCP dropped to >95%. The use of a precursor amount of 1000 nmol was exemplarily investigated on one compound, resulting in 36% yield (4% yield on the 100 nmol level, both yields uncorrected) (*12*). Another recently developed methodology allows for chemoselective transition-metal-assisted ^{18}F-deoxyfluorination of a tyrosine residue in small peptides (*14*). ^{18}F-deoxyfluorination of a series of small peptides was carried out using 5 µmol peptide precursor (corresponding to about 5-7.5 mg of typically used peptides of 1000-1500 g/mol) and a final HPLC purification within an overall synthesis time of 80-100 min. The authors described that reduction of the peptide amount to 1.5 µmol (1.5-2.3 mg) is possible, leading to a reduction of the RCY by about 50%, which corresponds to 10-20% RCY for the peptides used or 5-10% uncorrected yield 80-100 min after end-of-bombardment (*14*).

Regarding the Si-^{18}F bond formation initial experiments were performed with SiF_4 and alkyfluorosilanes in 1958 (*15-17*). In 2006, Schirrmacher et al. proved that sterically demanding substituents around the silicon (e.g. phenyls or branched alkyls) could preserve the Si-^{18}F bond and prevent fast hydrolysis in aqueous media (*6*). These results were supported by Blower et al. on ^{18}F-fluorination of alkoxysilanes in nucleophilic substitutions (*18*) and a systematic evaluation of different Silicon-Fluoride-Acceptor (SiFA) building blocks by Höhne et al. (*19*). A kinetic analysis for the isoenergetic replacement of ^{19}F by the PET-isotope ^{18}F in a SiFA moiety (*20*) revealed a low energy barrier of only 15.7 kcal/mol, which explains the fast ^{19}F-for-^{18}F IE reaction at r.t. within 5 min, yielding ^{18}F-SiFA-conjugated tracers in high yields (>40%) and high molar activities (>60 GBq/µmol). Moreover, the absence of side-products allows for a simple cartridge-based purification, resulting in a total synthesis time of <30 min (*21-23*).

In vivo studies in mice with ^{18}F-SiFA-TATE, an octreotate-based somatostatin receptor agonist, revealed no elevated activity accumulation in bone and thus high hydrolytic stability of the Si-^{18}F bond (*21,24*). However, due to the bulky and highly lipophilic SiFA, the activity was predominantly accumulating in the liver and gastrointestinal system (*21,24*). With the aim to increase hydrophilicity, incorporation of hydrophilic modifiers, such as carboxylic acids, carbohydrates, polyethylene glycol, and combinations thereof were tested (*21,22,25*). Moreover, a positive charge was introduced in the SiFA-building block (*20,21*). Despite the recent efforts to decrease the lipophilicity, none of the SiFA-bearing ligands described so far showed the potential for first proof-of-concept studies in men also necessary to confirm sufficient hydrolytic stability of the Si-^{18}F-bond in men.

To design SiFA-based prostate-specific membrane antigen (PSMA) inhibitors with sufficient hydrophilicity, we developed and investigated compounds that combine a SiFA moiety and a chelator (or chelate) in one single molecule, named radiohybridPSMA-inhibitors (rhPSMAs). Such rhPSMA-ligands can be a) labeled with ^{18}F by IE, while the chelator is used for complexation of a cold metal (e.g. ^{nat}Ga or ^{nat}Lu), or b) can be labeled with a radiometal (e.g. ^{68}Ga, ^{177}Lu or ^{225}Ac), while the SiFA moiety is non-radioactive (Figure 1). The new series of tracers was evaluated *in vitro* (IC_{50}, binding to and internalization into LNCaP cells, binding to human serum albumin (HSA)) and *in vivo* (LNCaP tumor-bearing SCID mice) and compared to the best recently described ^{18}F-labeled PSMA-inhibitors DCFPyL and PSMA-1007 (*26,27*).

MATERIALS AND METHODS

Chemical Synthesis

The rhPSMA-ligands were prepared *via* a mixed solid-phase/solution-phase synthetic strategy. Final purification of the compounds was achieved by reversed phase (RP) HPLC. A detailed description of the synthesis of uncomplexed rhPSMA-5 to 10 (see Supplemental Figure 1 to 12), including cold gallium complexation and their characterization is provided in the supplemental information. Structural formulas of

rhPSMAs and of the reference ligands, ^{nat}F-DCFPyL, ^{nat}F-PSMA-1007 and (((*S*)-1-carboxy-5-(4-(^{125}I-iodo)benzamido)pentyl)carbamoyl)-*L*-glutamic acid ((^{125}I-I-BA)KuE) are depicted in Figure 2 (*26-28*).

Radiolabeling

Automated ^{68}Ga-labeling. ^{68}Ga-labeling was performed using an automated system (GallElut^{+} by Scintomics, Germany) as described previously (*29*).

Manual ^{18}F-labeling. ^{18}F-Fluoride (approx. 0.6–2.0 GBq/mL) was provided by the *Klinikum rechts der Isar* (Munich, Germany). For manual ^{18}F-labeling a previously published procedure was slightly modified (*23*). Briefly, aqueous (aq.) $^{18}F^-$ was passed through a strong anion exchange cartridge (Sep-Pak Accell Plus QMA Carbonate Plus Light cartridge, 46 mg, 40 µm, Waters, Eschborn, Germany), which was preconditioned with 10 mL of water. Most of the remaining water was removed with 20 mL of air, and any residual was removed by rinsing the cartridge with 10 mL of anhydrous acetonitrile (for DNA synthesis, VWR, Darmstadt, Germany) followed by 20 mL air. For cartridge elution, $[K^+\subset 2.2.2]OH^-$ kits, containing a lyophilized mixture of 2.2.2-cryptand (Kryptofix® 222, 110 µmol, 1.1 eq., Sigma Aldrich, Germany) and KOH (100 µmol, 1.0 eq., 99.99% semiconductor grade, Sigma Aldrich) were used, which were dissolved in 500 µL of anhydrous acetonitrile prior to the elution process. The eluate was then partly neutralized with 30 µmol of oxalic acid (99.999%, trace metals basis, Sigma Aldrich) in anhydrous acetonitrile (1 M, 30 µL). The resulting mixture was used as a whole or aliquot for fluorination of 10-150 nmol of a respective labeling precursor 1 mM in anhydrous DMSO (>99.9 %, Sigma Aldrich) for 5 min at r.t. . For purification of the tracer, an Oasis HLB Plus Light cartridge (30 mg sorbent, 30 µm particle size, Waters), preconditioned with 10 mL of water was used. The labeling mixture was diluted with 9 mL phosphate buffered saline (PBS, pH 3, adjusted with 1 M aq. HCl) and passed through the cartridge followed by 10 mL PBS (pH 3) and 10 mL air. The peptide was eluted with 0.3–2.0 mL of a 1:1 mixture (*v*/*v*) of ethanol in water. RCP of the ^{18}F-labeled compound was determined by radio-TLC (Silica gel 60 RP-18 F_{254}s, mobile phase: 3:2 mixture (*v*/*v*) of acetonitrile in water supplemented with 10% of 2 M sodium acetate solution and 1% of trifluoroacetic acid) and radio RP-HPLC (Nucleosil 100 C18, 5 µm, 125 × 4.0 mm, mobile phases water and acetonitrile, both containing 0.1% trifluoroacetic acid (see supporting information).

Lipophilicity and Binding to Human Serum Albumin Approximately 1 MBq of the labeled tracer was dissolved in 1 mL of a 1:1 mixture (*v*/*v*) of PBS (pH 7.4) and *n*-octanol in a reaction vial (n=6). After vigorous mixing of the suspension for 3 min at r.t., the vial was centrifuged at 15,000×g for 3 min (Biofuge 15, Heraus Sepatech, Osterode, Germany) and 100 µL aliquots of both layers were measured in a gamma counter.

HSA binding of the rhPSMA-ligands was determined according to a previously published procedure via HPLC, using a Chiralpak HSA column (50 x 3 mm, 5 µm, H13H-2433, Daicel, Tokyo, Japan) with minor modifications (*30*).

In Vitro Experiments

Cell Culture. PSMA-positive LNCaP cells (300265; Cell Lines Service, Eppelheim, Germany) were cultivated in Dulbecco's modified Eagle medium/Nutrition Mixture F-12 with GlutaMAX (1:1, DMEM-F12, Biochrom, Germany) supplemented with fetal bovine serum (10%, FBS Zellkultur, Berlin, Germany) and kept at 37°C in a humidified CO_2 atmosphere (5%). A mixture of trypsin and ethylenediaminetetraacetic acid (0.05%, 0.02%) in PBS (Biochrom) was used in order to harvest cells. Cells were counted with a Neubauer hemocytometer (Paul Marienfeld, Lauda-Königshofen, Germany).

Affinity determinations (IC_{50}) and internalization studies. Competitive binding studies were determined on LNCaP cells (1.5×10^5 cells in 1 mL/well) after incubation at 4°C for one hour, using (^{125}I-I-BA)KuE (0.2 nM/well) as reference radioligand (n=3). Internalization studies of the radiolabeled ligands (0.5 nM/well) were performed on LNCaP cells (1.25×10^5 cells in 1 mL/well) at 37°C for one hour and accompanied by (^{125}I-I-BA)KuE (0.2 nM/well), as reference ligand. Data were corrected for non-specific binding and normalized to the specific-internalization observed for the radioiodinated reference compound (n=3).

In Vivo Experiments

All animal experiments were conducted in accordance with general animal welfare regulations in Germany (German animal protection act, as amended on 18.05.2018, Art. 141 G v. 29.3.2017 I 626, approval no. 55.2-1-54-2532-71-13) and the institutional guidelines for the care and use of animals. To

establish tumor xenografts, LNCaP cells (approx. 10^7 cells) were suspended in 200 µL of a 1:1 mixture (*v*/*v*) of DMEM F-12 and Matrigel (BD Biosciences, Germany), and inoculated subcutaneously onto the right shoulder of 6–8 weeks old CB17-SCID mice (Charles River, Germany). Mice were used for experiments when tumors had grown to a diameter of 5–10 mm (3–6 weeks after inoculation).

Biodistribution. Approximately 2–20 MBq (0.2 nmol) of the radioactive-labeled PSMA-inhibitors were injected into the tail vein of LNCaP tumor-bearing male CB-17 SCID mice that were sacrificed after 1 h post injection (p.i.) (n=3 for ^{68}Ga-^{19}F-rhPSMA-7 to 9 and ^{18}F-rhPSMA-7, n=4 for ^{68}Ga-^{19}F-rhPSMA-10, ^{18}F-DCFPyL and ^{18}F-PSMA-1007). Selected organs were removed, weighted and measured in a gamma counter.

RESULTS

Synthesis and Radiolabeling

Synthesis of uncomplexed rhPSMA-5 to 10 was carried out *via* a straightforward mixed solid phase/solution phase synthetic strategy (see supplemental information).

Final products were obtained in a chemical purity of >97%, determined by HPLC (220 nm). Cold metal complexation with molar excess of $Ga(NO_3)_3$: 1.5-fold molar excess for 1,4,7-triazacyclononane-1,4,7-tris[methyl(2-carboxyethyl)phosphinic acid] (TRAP)-based conjugates, 3.0-fold molar excess for 1,4,7,10-Tetraazacyclododecane-1,4,7,10-tetraacetic acid (DOTA)-based conjugates lead to a quantitative formation of the respective ^{nat}Ga-rhPSMA-ligand (Figure 2).

^{68}Ga-labeling of uncomplexed rhPSMA was performed in a standard automated procedure in RCYs of 60 ± 7% and molar activities of 59 ± 20 GBq/µmol. RCPs were >97% for all compounds.

^{18}F-labeling was carried out by ^{19}F/^{18}F IE reaction already described for SiFA-compounds in a manual procedure (*23*). Drying of aq. ^{18}F-fluoride was performed through ^{18}F-fixation on a strong anion exchange cartridge (QMA, Waters), followed by removal of water with air and anhydrous acetonitrile, according to the previously described *Munich Method (31)*. Dried ^{18}F-fluoride was eluted from the QMA by $[K^+\subset 2.2.2]OH^-$ directly into a mixture of the labeling precursor and oxalic acid in 150 µL DMSO and

30 µL MeCN (recovery of ^{18}F-fluoride >95%). The IE reaction was completed in 5 min at r.t.. Due to the chemical identity of the starting material and radiolabeled product and the absence of chemical side-products, a cartridge-based purification yielded the purified ligand in a total synthesis time of approximately 20 min in a RCP of >97%. The ^{18}F-rhPSMA-ligands could be obtained in RCYs of 58 ± 9% (n=11, 50-150 nmol precursor) and molar activities of 12–60 GBq/µmol, when using starting activities of 0.2–9.0 GBq (exemplary HPLC analysis is shown in Supplemental Figure 13).

In Vitro Characterization

In vitro data of the synthesized (radio)metal-chelated rhPMSA ligands are summarized in Figure 3 and Supplemental Table 1; data from the well-established fluorinated PSMA-ligands DCFPyL and PSMA-1007, evaluated under the same experimental conditions, were taken from a previously published study by our group and are included for comparison (*26,27,32*). Due to the chemical identity of the ^{68}Ga-^{19}F-rhPSMA with the respective ^{nat}Ga-^{18}F-rhPSMA compound, only the ^{68}Ga-labeled twin was evaluated in experiments that required a radioactive compound. Moreover, the uncomplexed ^{18}F-labeled rhPSMA-ligands were tested in order to assess the influence of the chelated metal cation on the *in vitro* behavior.

The PSMA binding affinities (IC_{50}) (Figure 3, A) were determined in a competitive binding assay on LNCaP human prostate carcinoma cells, using (^{125}I-I-BA)KuE, as radioligand. rhPSMA-5 and 6 that are based on the Lys-urea-Glu (KuE) scaffold, showed PSMA affinities somewhat better than that obtained for ^{19}F-DCFPyL. Higher PSMA affinities were measured for the reference ligand ^{19}F-PSMA-1007 and the Glu-urea-Glu-(EuE-)-based inhibitors rhPSMA-7 to rhPSMA-10. For the individual rhPSMA-inhibitors in their Ga-complexed and metal-free forms similar IC_{50}s were found.

The extent of internalization was determined for each ^{68}Ga-^{19}F-rhPSMA compound and uncomplexed ^{18}F-rhPSMA-7 to 9 on LNCaP cells (1 h, 37°C) and normalized to the specific internalization of the reference radioligand (^{125}I-I-BA)KuE, which was assayed in a parallel experiment for each study (Figure 3, B). Compared with the KuE-based rhPSMAs and corresponding with the trend observed in the affinity studies, internalization was considerably higher for all EuE-motif based rhPSMA-inhibitors.

Especially the uncomplexed ^{18}F-fluorinated rhPSMA-ligands displayed higher internalization rates as determined for the Ga-chelated analogues and also the reference ligands, ^{18}F-DCFPyL and ^{18}F-PSMA-1007.

For all newly developed rhPSMA-inhibitors, partition-coefficients (log $P_{oct/PBS}$, pH 7.4) between -2.0 and -3.5 were determined (Figure 3, C). Interestingly, unchelated ^{18}F-labeled compounds, when compared with the Ga-complexed counterparts, exhibited higher lipophilicity. A similar high hydrophilicity was determined for ^{18}F-DCFPyL (-3.4), whereas ^{18}F-PSMA-1007 was found to be of rather lipophilic nature (-1.6).

Binding to HSA was assessed by means of a recently described HPLC method (Figure 3, D) (*30*). Despite their high hydrophilicity all SiFA-containing ligands exhibited strong HSA interactions with binding >94% (^{19}F-PSMA-1007 and ^{19}F-DCFPyL: 98% and 14% HSA binding, respectively).

In Vivo Characterization

Taking into account the results of the *in vitro* assessment, only the EuE-based ligands ^{68}Ga-^{19}F-rhPSMA-7 to 10 were evaluated in biodistribution studies in male LNCaP tumor-bearing CB17 SCID mice at 1 h p.i. and compared to the biodistribution of ^{18}F-DCFPyL and ^{18}F-PSMA-1007 (Figure 4 and Supplemental Table 2) (*32*).

The comparative biodistribution study revealed that all of the examined ligands displayed similar pharmacokinetics with high uptake in PSMA-expressing tissue, e.g. LNCaP tumors and kidneys, and in spleen and adrenal gland. Compared with the fluorinated reference ligands, tumor uptake at 1 h p.i. was similar for ^{18}F-DCFPyL, ^{18}F-PSMA-1007, ^{68}Ga-^{19}F-rhPSMA-7, 8 and 9 and somewhat higher for ^{68}Ga-^{19}F-rhPSMA-10. Non-target accumulation was low for all tracers with fast clearance *via* the renal pathway, except for ^{18}F-PSMA-1007, which showed higher uptake in a variety of organs, such as the gastrointestinal system, but also lung and pancreas. Compared with all other tracers, ^{18}F-DCPFyL and ^{68}Ga-^{19}F-rhPSMA-9 were more rapidly cleared from the blood within 1 h p.i..

Biodistribution of ^{68}Ga-^{19}F-rhPSMA-7 and ^{18}F-rhPSMA-7

The biodistributions of uncomplexed ^{18}F-rhPSMA-7 and ^{68}Ga-labeled ^{19}F-rhPSMA-7 were compared in order to examine the influence of the presence of the free chelator and a (radio-)metal chelate on the *in vivo* behavior in male, LNCaP tumor-bearing SCID mice at 1 h p.i. (Figure 5 and Supplemental Table 2).

The uptake profiles of ^{68}Ga-^{19}F-rhPSMA-7 and unmetalated ^{18}F-rhPSMA-7 in mice were found to be quite identical, with similar low uptake in most organs and pronounced uptake in spleen, kidneys, adrenal gland and tumor tissue. Although marked differences were found in the kidneys, in which the uncomplexed ^{18}F-labeled ligand displayed stronger accumulation (72 vs. 34% ID/g; injected dose per gram), it remains questionable, whether this difference is representative for the application in men. Interestingly, when compared with uncomplexed ^{18}F-rhPSMA-7, a 1.6-fold higher tumor uptake was found for ^{68}Ga-^{19}F-rhPSMA-7. Again, no elevated bone accumulation was found for ^{18}F-rhPSMA-7, indicating the absence of free ^{18}F-fluoride.

DISCUSSION

With the aim to develop a ^{18}F-labeled PSMA-targeted inhibitor with excellent labeling and thus production properties, we combined for the very first time a chelator and a SiFA moiety in one single inhibitor. Although the initial premise of this concept was driven by the expectation that a chelator (or a chelate) will significantly improve the hydrophilicity of the resulting SiFA-based tracer, a number of additional advantages of this radiohybrid concept became apparent. First, both the SiFA and the chelator can be labeled in an independent manner by using the unprotected precursor, resulting in either ^{18}F-M-rhPSMA (M=metal) or ^{19}F-R-rhPSMA (R=radiometal), the latter to be used for imaging (e.g. ^{68}Ga for PET, ^{111}In for SPECT or ^{177}Lu for therapy). The corresponding radiopharmaceuticals, e.g. ^{18}F-^{nat}Ga-rhPSMA or ^{19}F-^{68}Ga-rhPSMA, are chemically identical molecules. Thus, they represent “chemical monozygotic twins” that can be used with one of the two corresponding radioisotopes, but should result in almost identical PET scans, with only slight differences determined by the nuclear properties of the chosen radioisotope. In

addition, when using ^{18}F in combination with a therapeutic radioisotope, such as ^{177}Lu, the resulting twins, ^{18}F-^{nat}Lu-rhPSMA or ^{19}F-^{177}Lu-rhPSMA, could for the very first time truly bridge ^{18}F-PET and radioligand therapy. Although speculative, such tracers might be interesting tools for pretherapeutic patient stratification, pretherapeutic dosimetry and radioligand therapy with one single tracer by exploiting ^{18}F and the most suitable therapeutic radioisotope (if also available as non-radioactive isotope).

Thus, and with great enthusiasm, we developed and evaluated a series of PSMA targeted radiohybrid inhibitors. By slightly modifying the ^{18}F-labeling procedure for IE on SiFA moieties (*23*), ^{18}F-rhPSMA-ligands could be obtained in manual laboratory experiments in up 58% RCY, with molar activities of up to 60 GBq/µmol, similar to those reported in previous works of SiFA-bearing compounds (*21-24*). The combination of a) the *Munich Drying Method*, which comprises a simple and fast drying of aq. ^{18}F-fluoride on a solid-phase and the subsequent elution of dry ^{18}F-fluoride (*31*), b) the rapid and efficient ^{18}F-for-^{19}F IE at r.t. and c) the possibility to purify the final product by solid-phase extraction, resulted in a fast, but still not optimized, non-automated production that was completed in less than 20 min with RCY of about 55% (not optimized) and RCP >97%.

In the context of SiFA-conjugated ligands we were able to overcome the previously unresolved lipophilicity problem. Even the incorporation of more or less complex combinations of hydrophilic auxiliaries could not compensate for the pronounced lipophilic influence of the SiFA-group (log P SiFA-lin-TATE = -1.21 (*21*); log P Ga-DOTATATE= -3.69 (*33*)) and the associated unsuitable biodistribution of such conjugates, a main obstacle for proof-of-concept studies in men. As described here, a chelator or a related metal chelate, conjugated in close proximity to a SiFA moiety of a rhPSMA-ligand, increases the overall hydrophilicity of the inhibitor, while SiFA as lipophilic moiety and HSA binder decelerates blood clearance kinetics and avoids rapid and extensive occurrence of activity in the bladder. All rhPSMAs showed log P values between -2.0 and -3.5 (Figure 3, C) and thus exceeded the hitherto lowest lipophilicity of a SiFA-based ligand described in literature, an $\alpha_v\beta_3$ integrin-binding RGD-peptide with a log P of -2.0 (*22*). Interestingly, the Ga-chelated rhPSMA-ligands displayed a higher hydrophilicity, compared with the

respective uncomplexed analogues, even though their carboxylates are coordinated to the metal ion. Whether this unexpected observation is a general characteristic of rhPSMA is still under investigation.

Less surprising, and when compared with the KuE-based inhibitors rhPSMA-5 and 6, the EuE-rhPSMAs-7 to 10 showed improved PSMA binding affinities (IC_{50}s) and internalization rates, which were, compared to the reference ligands ^{18}F-DCFPyL and ^{18}F-PSMA-1007, similar or even better. The superiority of EuE-based inhibitors derivatized in the same manner as described for rhPSMA-7 to 10 has been previously reported in a detailed study on the structure-activity relationship of EuE- and KuE

-based PSMA-inhibitors conducted by Babich and co-workers (*34*). In a series of otherwise identical PSMA-inhibitors, Glu(Lys(R))-urea-Glu based inhibitors, comprising of a free carboxylate (of Lys) in close proximity to the inhibitor motif, showed the highest affinities. The authors speculated that the EuE motif and the free carboxylate of Lys may increase the ligand interaction with PSMA (*34*). Regarding unspecific uptake in non-target tissues and organs, all rhPSMA and both fluorinated reference ligands showed similar uptake profiles in most tissues. Most probably as a result of their high HSA binding and low lipophilicity, the blood levels at 1 h p.i. were generally slightly higher for rhPSMA-ligands, whereas the liver uptakes were lower compared to the reference ligands. Not unexpectedly, the most lipophilic tracer in this study, ^{18}F-PSMA-1007 (log P = -1.6), showed the highest uptake in almost all organs and tissues.

Since the internalizations of uncomplexed ^{18}F-labeled ligands were superior to the respective Ga-chelated counterpart (Figure 3, B), the biodistribution profiles of ^{68}Ga-^{19}F-rhPSMA-7 and ^{18}F-rhPSMA-7 with free 2-(4,7,10-tris(carboxymethyl)-1,4,7,10-tetraazacyclododecan-1-yl)pentanedioic acid (DOTAGA) chelator were also compared. Although the *in vitro* parameters seem to favor ^{18}F-rhPSMA-7, the tumor uptake of the uncomplexed ligand was unexpectedly low, despite its 1.3-fold higher internalization and comparable PSMA affinity. The exact reason for this finding remains unclear and needs further investigation. The additional free carboxylic acids of the uncomplexed ^{18}F-rhPSMA-7 inhibitor also accounted for a 2-fold increased kidney uptake, again demonstrating the negative influence of charges on tracer uptake in the kidneys (*35-37*).

After completion of this study, an automated production of ^{18}F-rhPSMA-7 has been successfully developed and established at the Department of Nuclear Medicine, Technical University of Munich and Department of Nuclear Medicine, Ludwig Maximilians University Munich. The results and experience gained from almost 400 routine productions will be described elsewhere. Results on the first clinical evaluation of ^{18}F-rhPSMA-7 are described in this issue of the Journal of Nuclear Medicine by Oh et al. (38), Eiber et al. (39) and Kroenke et al. (40).

In summary we could demonstrate that rhPSMA-inhibitors, as a first series of radiopharmaceuticals developed under the radiohybrid concept, are powerful new inhibitors with equal or even better targeting characteristics than the established ^{18}F-PSMA tracers DCFPyL and PSMA-1007. Moreover, such radiohybrids offer the possibility to produce the identical ^{68}Ga-labeled ^{19}F-^{68}Ga-rhPSMA tracers at sites that favor ^{68}Ga-labeling, and the possibility to extend this concept to theranostic radiohybrid radiopharmaceuticals, such as F-Lu-rhPSMA.

CONCLUSION

Taking into account the results of the above mentioned comparative assessment, the development of an automated production of the F-Ga-rhPSMA-7 and F-Ga-rhPSMA-10 is highly warranted and a prerequisite to assess the clinical value of the first ^{18}F-rhPSMAs in proof-of-concept studies in men.

DISCLOSURE

Patent application for rhPSMA (HJW, AW and ME). ME and HJW receive funding from the SFB 824 (DFG Sonderforschungsbereich 824, Project B11); HJW receives funding from the SFB 824, Project Z) from the Deutsche Forschungsgemeinschaft, Bonn, Germany. ME received funding from Blue Earth Diagnostics Ltd (licensee for rhPSMA) as part of an academic collaboration and is consultant for Blue Earth Diagnostics Ltd.. HJW is founder, shareholder and scientific advisor of Scintomics GmbH, Fuerstenfeldbruck, Germany. No other potential conflicts of interest relevant to this article exist.

ACKNOWLEDGMENTS

We thank the GMP-production team at the Departments of Nuclear Medicine at the Technical University of Munich for routine delivery of ^{18}F-fluoride and C.Turnbull, R.Bejot and M.F.Fahnauer for carefully proofreading the manuscript.

KEY POINTS

QUESTION: Is it possible to design a SiFA-conjugated PSMA-inhibitor with promising characteristics by introduction of a chelate into the same molecule?

PERTINENT FINDINGS: Especially ^{18}F-^{nat}Ga-rhPSMA-7 meets all major preclinical and pharmaceutical requirements for a first assessment in humans.

IMPLICATIONS FOR PATIENT CARE: Although the diagnostic value of ^{18}F-^{nat}Ga-rhPSMA-7 has to be confirmed in clinical studies, this study on rhPSMAs and the entire radiohybrid concept could open new perspectives in prostate cancer theranostics.

REFERENCES

1. Schwaiger M, Wester HJ. How many PET tracers do we need? *J Nucl Med.* 2011;52 Suppl 2:36s-41s.

2. Maecke HR, André JP. ^{68}Ga-PET radiopharmacy: A generator-based alternative to ^{18}F-radiopharmacy. *Ernst Schering Res Found Workshop.* 2007:215-242.

3. Dornan MH, Simard JM, Leblond A, et al. Simplified and robust one-step radiosynthesis of [^{18}F]DCFPyL via direct radiofluorination and cartridge-based purification. *J Labelled Comp Radiopharm.* 2018;61:757-763.

4. Bouvet V, Wuest M, Jans HS, et al. Automated synthesis of [^{18}F]DCFPyL via direct radiofluorination and validation in preclinical prostate cancer models. *EJNMMI Res.* 2016;6:40.

5. Cardinale J, Martin R, Remde Y, et al. Procedures for the GMP-compliant production and quality control of [^{18}F]PSMA-1007: A next generation radiofluorinated tracer for the detection of prostate cancer. *Pharmaceuticals (Basel).* 2017;10.

6. Schirrmacher R, Bradtmöller G, Schirrmacher E, et al. ^{18}F-labeling of peptides by means of an organosilicon-based fluoride acceptor. *Angew Chem Int Ed Engl.* 2006;45:6047-6050.

7. Ting R, Adam MJ, Ruth TJ, Perrin DM. Arylfluoroborates and alkylfluorosilicates as potential PET imaging agents: high-yielding aqueous biomolecular ^{18}F-labeling. *J Am Chem Soc.* 2005;127:13094-13095.

8. McBride WJ, Sharkey RM, Karacay H, et al. A novel method of ^{18}F radiolabeling for PET. *J Nucl Med.* 2009;50:991-998.

9. Laverman P, McBride WJ, Sharkey RM, et al. A novel facile method of labeling octreotide with ^{18}F-fluorine. *J Nucl Med.* 2010;51:454-461.

10. Liu T, Liu C, Xu X, et al. Preclinical evaluation and pilot clinical study of Al^{18}F-PSMA-BCH for prostate cancer PET imaging. *J Nucl Med.* 2019;60:1284-1292.

11. Liu Z, Pourghiasian M, Radtke MA, et al. An Organotrifluoroborate for broadly applicable one-step ^{18}F-labeling. *Angew Chem Int Ed Engl.* 2014;53:11876-11880.

12. Kuo HT, Lepage M, Lin KS, et al. One-step ^{18}F-labeling and preclinical evaluation of prostate specific membrane antigen trifluoroborate probes for cancer imaging. *J Nucl Med.* 2019;60:1160-1166.

13. Ting R, Harwig C, auf dem Keller U, et al. Toward [^{18}F]-labeled aryltrifluoroborate radiotracers: In vivo positron emission tomography imaging of stable aryltrifluoroborate clearance in mice. *J Am Chem Soc.* 2008;130:12045-12055.

14. Rickmeier J, Ritter T. Site-specific deoxyfluorination of small peptides with [^{18}F]Fluoride. *Angew Chem Int Ed Engl.* 2018;57:14207-14211.

15. Gens TA, Wethongton JA, Brosi AR. The exchange of F18 between metallic fluorides and silicon tetrafluoride. *J Phys Chem.* 1958;62:1593-1593.

16. Poole RT, Winfield JM. Radiotracers in fluorine chemistry. Part IV. Fluorine-18 exchange between labelled alkylfluorosilanesand fluorides, or fluoride methoxides, of tungsten(VI), molybdenum(VI), tellurium(VI), and iodine(V). *Dalton Trans.* 1976:1557-1560.

17. Winfield JM. Preparation and use of 18-fluorine labelled inorganic compounds. *J Fluor Chem.* 1980;16:1-17.

18. Choudhry U, Martin KE, Biagini S, Blower PJ. A49 Alkoxysilane groups for instant labelling of biomolecules with ^{18}F. *Nucl Med Commun.* 2006;27:293.

19. Höhne A, Yu L, Mu L, et al. Organofluorosilanes as model compounds for ^{18}F-labeled silicon-based PET tracers and their hydrolytic stability: experimental data and theoretical calculations (PET = positron emission tomography). *Chemistry.* 2009;15:3736-3743.

20. Kostikov AP, Iovkova L, Chin J, et al. N-(4-(di-tert-butyl[^{18}F]fluorosilyl)benzyl)-2-hydroxy-N,N-dimethylethylammonium bromide ([^{18}F]SiFAN+Br−): A novel lead compound for the development of hydrophilic SiFA-based prosthetic groups for 18F-labeling. *J Fluor Chem.* 2011;132:27-34.

21. Niedermoser S, Chin J, Wängler C, et al. In vivo evaluation of ^{18}F-SiFAlin-modified TATE: A potential challenge for ^{68}Ga-DOTATATE, the clinical gold standard for somatostatin receptor imaging with PET. *J Nucl Med.* 2015;56:1100-1105.

22. Lindner S, Michler C, Leidner S, et al. Synthesis and in vitro and in vivo evaluation of SiFA-tagged bombesin and RGD peptides as tumor imaging probes for positron emission tomography. *Bioconjug Chem.* 2014;25:738-749.

23. Wängler C, Niedermoser S, Chin J, et al. One-step ^{18}F-labeling of peptides for positron emission tomography imaging using the SiFA methodology. *Nat Protoc.* 2012;7:1946-1955.

24. Wängler C, Waser B, Alke A, et al. One-step ^{18}F-labeling of carbohydrate-conjugated octreotate-derivatives containing a silicon-fluoride-acceptor (SiFA): In vitro and in vivo evaluation as tumor imaging agents for positron emission tomography (PET). *Bioconjugate Chem.* 2010;21:2289-2296.

25. Litau S, Niedermoser S, Vogler N, et al. Next generation of SiFAlin-based TATE derivatives for PET imaging of SSTR-positive tumors: Influence of molecular design on in vitro SSTR binding and in vivo pharmacokinetics. *Bioconjug Chem.* 2015;26:2350-2359.

26. Chen Y, Pullambhatla M, Foss CA, et al. 2-(3-{1-Carboxy-5-[(6-[^{18}F]fluoro-pyridine-3-carbonyl)-amino]-pentyl}-ureido)-pen tanedioic acid, [^{18}F]DCFPyL, a PSMA-based PET imaging agent for prostate cancer. *Clin Cancer Res.* 2011;17:7645-7653.

27. Cardinale J, Schäfer M, Benešová M, et al. Preclinical evaluation of ^{18}F-PSMA-1007, a new prostate-specific membrane antigen ligand for prostate cancer imaging. *J Nucl Med.* 2017;58:425-431.

28. Weineisen M, Simecek J, Schottelius M, Schwaiger M, Wester HJ. Synthesis and preclinical evaluation of DOTAGA-conjugated PSMA ligands for functional imaging and endoradiotherapy of prostate cancer. *EJNMMI Res.* 2014;4:63.

29. Notni J, Pohle K, Wester HJ. Comparative gallium-68 labeling of TRAP-, NOTA-, and DOTA-peptides: practical consequences for the future of gallium-68-PET. *EJNMMI Res.* 2012;2:28.

30. Valko K, Nunhuck S, Bevan C, Abraham MH, Reynolds DP. Fast gradient HPLC method to determine compounds binding to human serum albumin. Relationships with octanol/water and immobilized artificial membrane lipophilicity. *J Pharm Sci.* 2003;92:2236-2248.

31. Wessmann SH, Henriksen G, Wester HJ. Cryptate mediated nucleophilic ^{18}F-fluorination without azeotropic drying. *Nuklearmedizin.* 2012;51:1-8.

32. Robu S, Schmidt A, Eiber M, et al. Synthesis and preclinical evaluation of novel ^{18}F-labeled Glu-urea-Glu-based PSMA inhibitors for prostate cancer imaging: a comparison with ^{18}F-DCFPyl and ^{18}F-PSMA-1007. *EJNMMI Res.* 2018;8:30.

33. Schottelius M, Šimeček J, Hoffmann F, Willibald M, Schwaiger M, Wester HJ. Twins in spirit - episode I: comparative preclinical evaluation of [^{68}Ga]DOTATATE and [^{68}Ga]HA-DOTATATE. *EJNMMI Res.* 2015;5:22.

34. Lu G, Maresca KP, Hillier SM, et al. Synthesis and SAR of ^{99m}Tc/Re-labeled small molecule prostate specific membrane antigen inhibitors with novel polar chelates. *Bioorg Med Chem Lett.* 2013;23:1557-1563.

35. Béhé M, Kluge G, Becker W, Gotthardt M, Behr TM. Use of polyglutamic acids to reduce uptake of radiometal-labeled minigastrin in the kidneys. *J Nucl Med.* 2005;46:1012-1015.

36. Gotthardt M, van Eerd-Vismale J, Oyen WJ, et al. Indication for different mechanisms of kidney uptake of radiolabeled peptides. *J Nucl Med.* 2007;48:596-601.

37. Eder M, Löhr T, Bauder-Wüst U, et al. Pharmacokinetic properties of peptidic radiopharmaceuticals: reduced uptake of $(EH)_3$-conjugates in important organs. *J Nucl Med.* 2013;54:1327-1330.

38. Oh SW, Wurzer A, Teoh E, et al. Quantitative and qualitative analyses of biodistribution and PET image quality of novel radiohybrid PSMA, ^{18}F-rhPSMA-7, in patients with prostate cancer. Manuscript number: JNUMED/2019/234609.

39. Eiber M, Kroenke M, Wurzer A, et al. ^{18}F-rhPSMA-7 positron emission tomography for the detection of biochemical recurrence of prostate cancer following radical prostatectomy. Manuscript number: JNUMED/2019/234914.

40. Kroenke M, Wurzer A, Schwamborn K, et al. Histologically-confirmed diagnostic efficacy of ^{18}F-rhPSMA-7 positron emission tomography for N-staging of patients with primary high-risk prostate cancer. Manuscript number: JNUMED/2019/234906.

Legend to Figures:

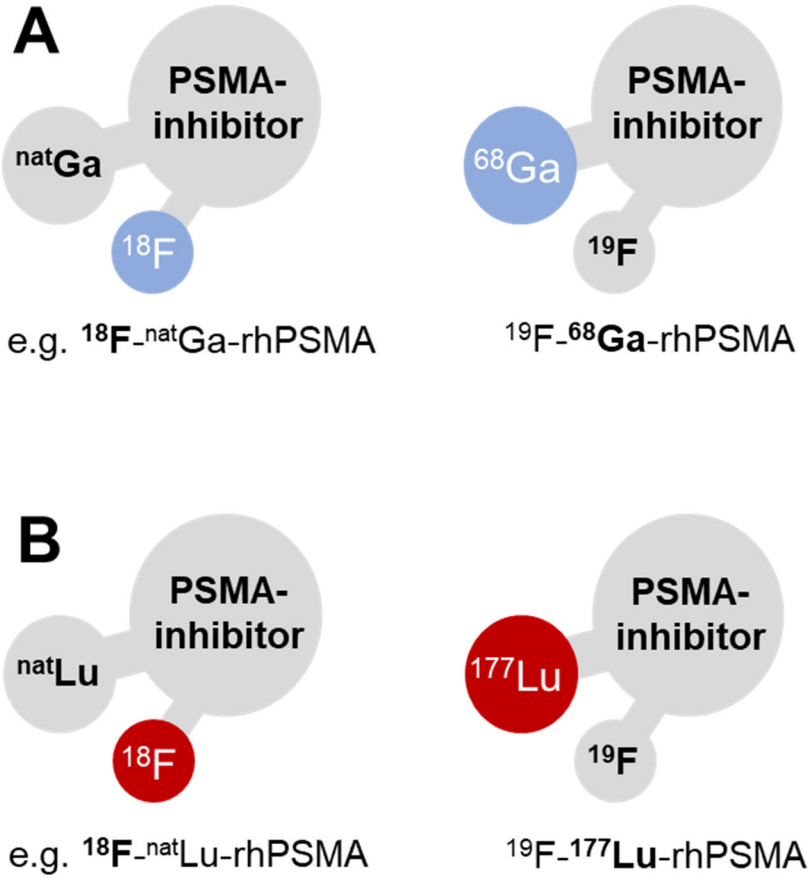

FIGURE 1. The radiohybrid concept exemplified on PSMA-inhibitors: a molecular species that offers two binding sites for radionuclides, here a Silicon-Fluoride-Acceptor (SiFA) for ^{18}F and a chelate for radiometallation. One of these binding sites is "labeled" with a radioisotope, the other one is silent, thus "labeled" with a nonradioactive isotope. These pair of compounds, either pure imaging pairs (A) or theranostic pairs (B) represent chemically identical species (monozygotic chemical twins) and thus exhibit identical *in vivo* characteristics (affinity, lipophilicity, pharmacokinetics etc.). Note: ^{68}Ga in (A) and ^{177}Lu in (B) are examples that can be substituted by other (radio-)metals.

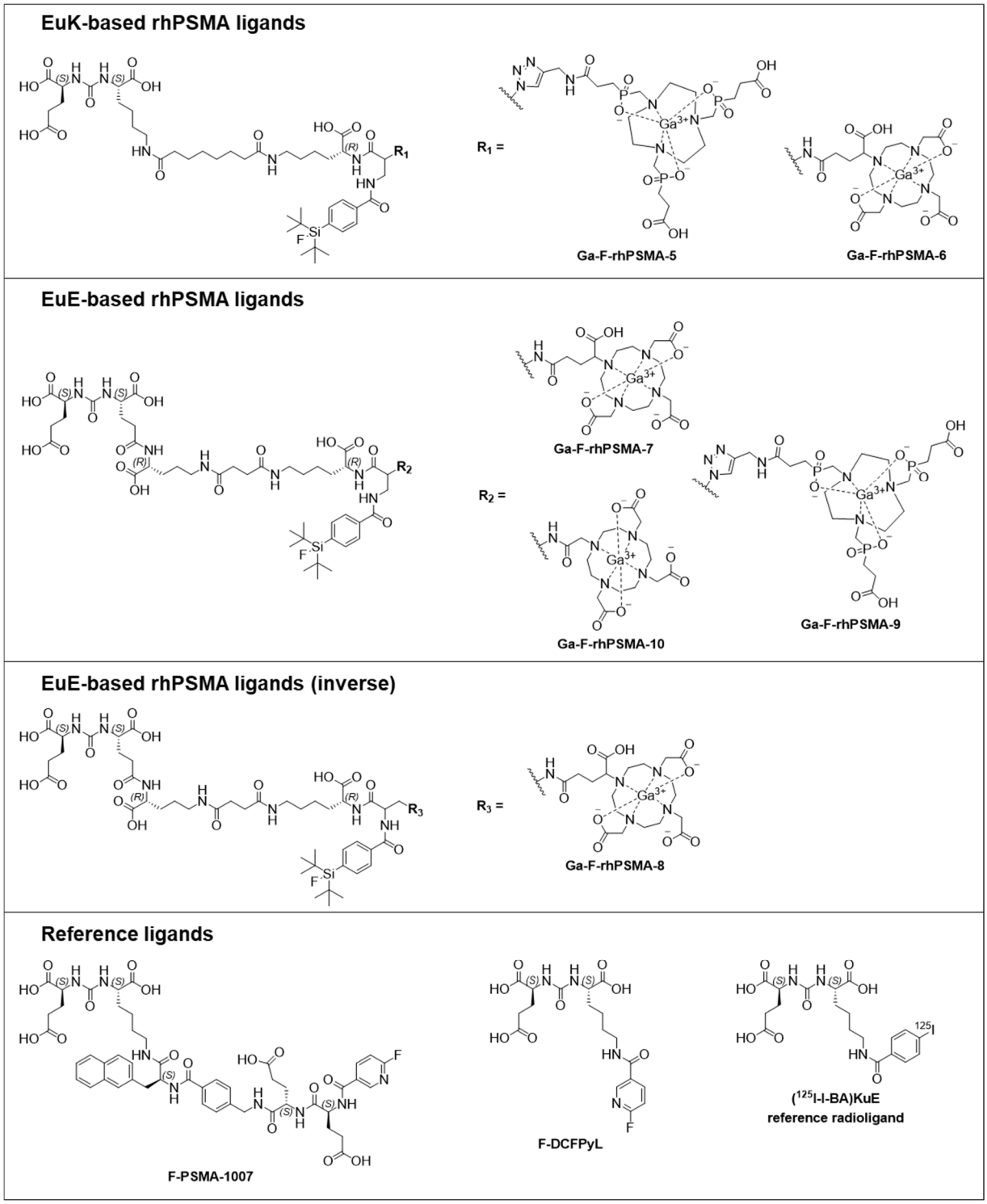

FIGURE 2. Radiohybrid (rh) PSMA-ligands comprising of the KuE- or EuE-based PSMA inhibition motif, a SiFA moiety and a TRAP-, DOTA- or DOTAGA-chelator. For comparative evaluations the well-established PSMA-addressing ligands, F-PSMA-1007 and F-DCFPyL were used (*26,27*). The reference radioligand for *in vitro* determinations was (^{125}I-I-BA)KuE (*28*).

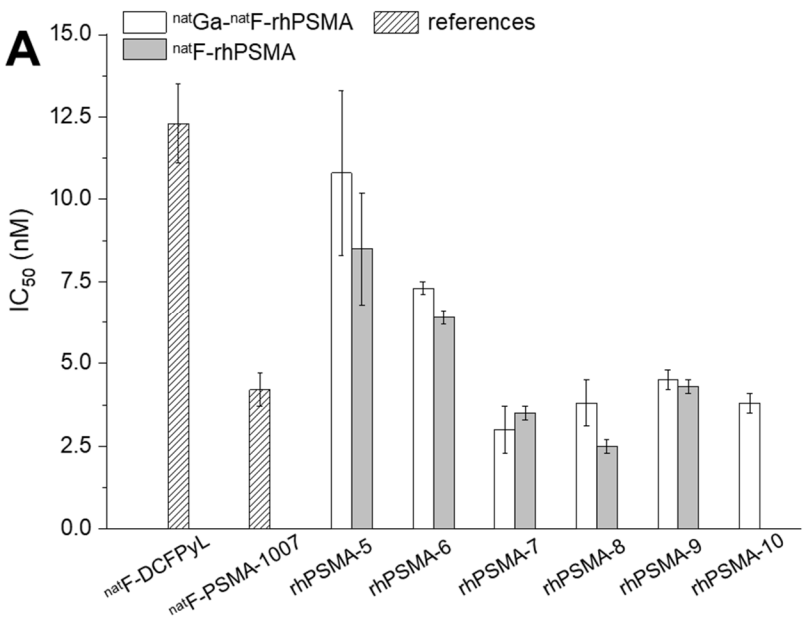
A
natGa-natF-rhPSMA
natF-rhPSMA
references
IC50 (nM)
15.0
12.5
10.0
7.5
5.0
2.5
0.0
natF-DCFPyL
natF-PSMA-1007
rhPSMA-5
rhPSMA-6
rhPSMA-7
rhPSMA-8
rhPSMA-9
rhPSMA-10

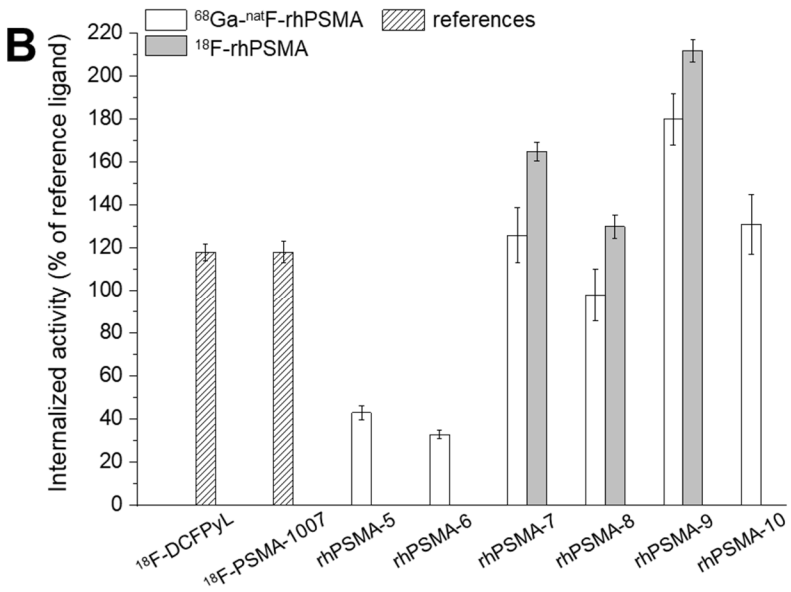
B
68Ga-natF-rhPSMA
18F-rhPSMA
references
Internalized activity (% of reference ligand)
220
200
180
160
140
120
100
80
60
40
20
0
18F-DCFPyL
18F-PSMA-1007
rhPSMA-5
rhPSMA-6
rhPSMA-7
rhPSMA-8
rhPSMA-9
rhPSMA-10

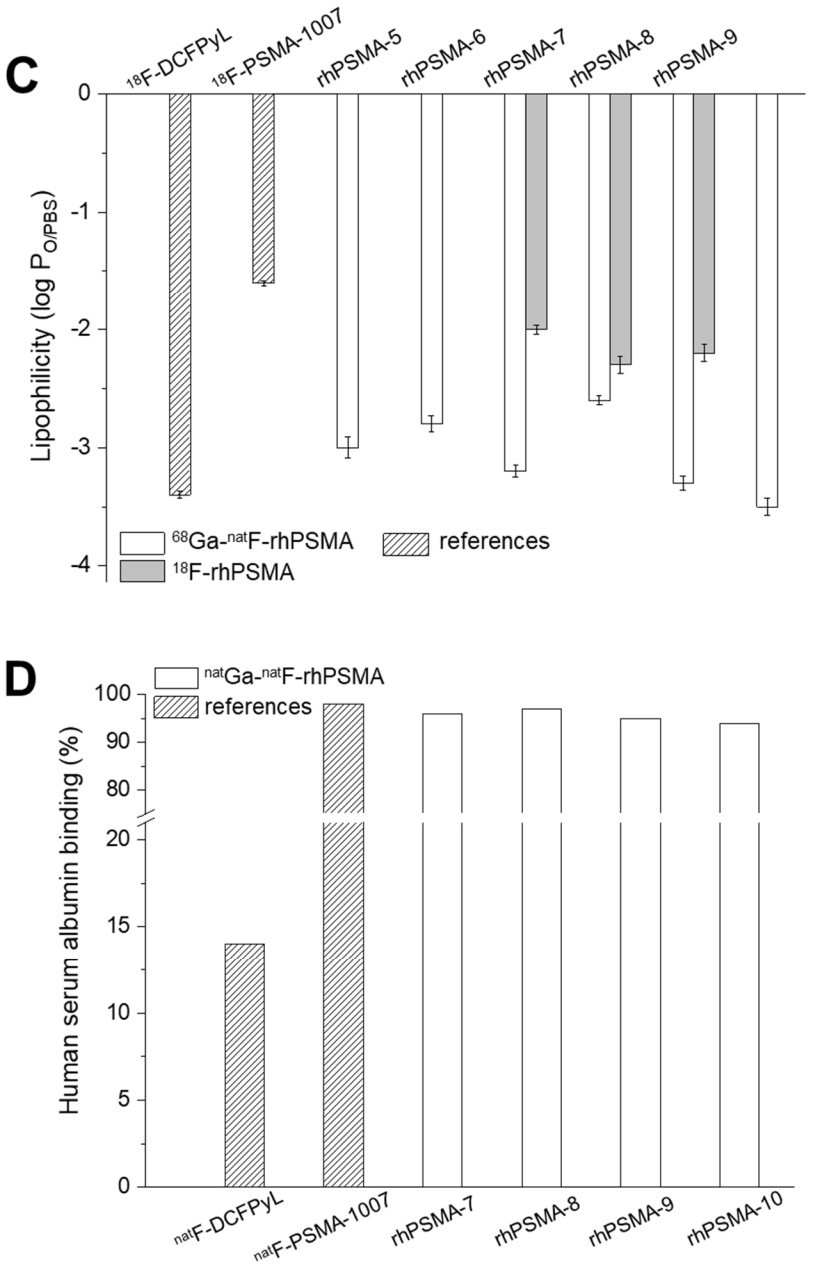

FIGURE 3. **A**) Binding affinities (IC_{50} in nM, 1 h, 4°C; n=3) of ^{nat}Ga-^{19}F-rhPSMA-5–10 (white bars), ^{19}F-rhPSMA-5–10 with free chelator (grey bars), ^{19}F-DCFPyL and ^{19}F-PSMA-1007; **B**) internalized activity of ^{18}F-DCFPyL, ^{18}F-PSMA-1007, ^{68}Ga-^{19}F-rhPSMA-5–10 (white bars) and ^{18}F-rhPSMA-5–10 with free chelator (grey bars), in LNCaP cells (1 h, 37°C) as percent of the reference ligand (^{125}I-I-BA)KuE; n=3); **C**) lipophilicity of ^{18}F-DCFPyL, ^{18}F-PSMA-1007, ^{68}Ga-^{19}F-rhPSMA-5–10 (white bars) and ^{18}F-rhPSMA-5–10 with free chelator (grey bars), expressed as *n*-octanol/PBS (pH 7.4) partition-coefficient (log $P_{oct/PBS}$; n=6); **D**) human serum albumin

binding of ^{19}F-DCFPyL, ^{19}F-PSMA-1007, ^{nat}Ga-^{19}F-rhPSMA-5–10 (white bars), determined on a Chiralpak HSA column. Data of reference ligands $^{18/19}$F-DCFPyL and $^{18/19}$F-PSMA-1007 from a previously published study (*32*). Values are expressed as mean ± standard deviation.

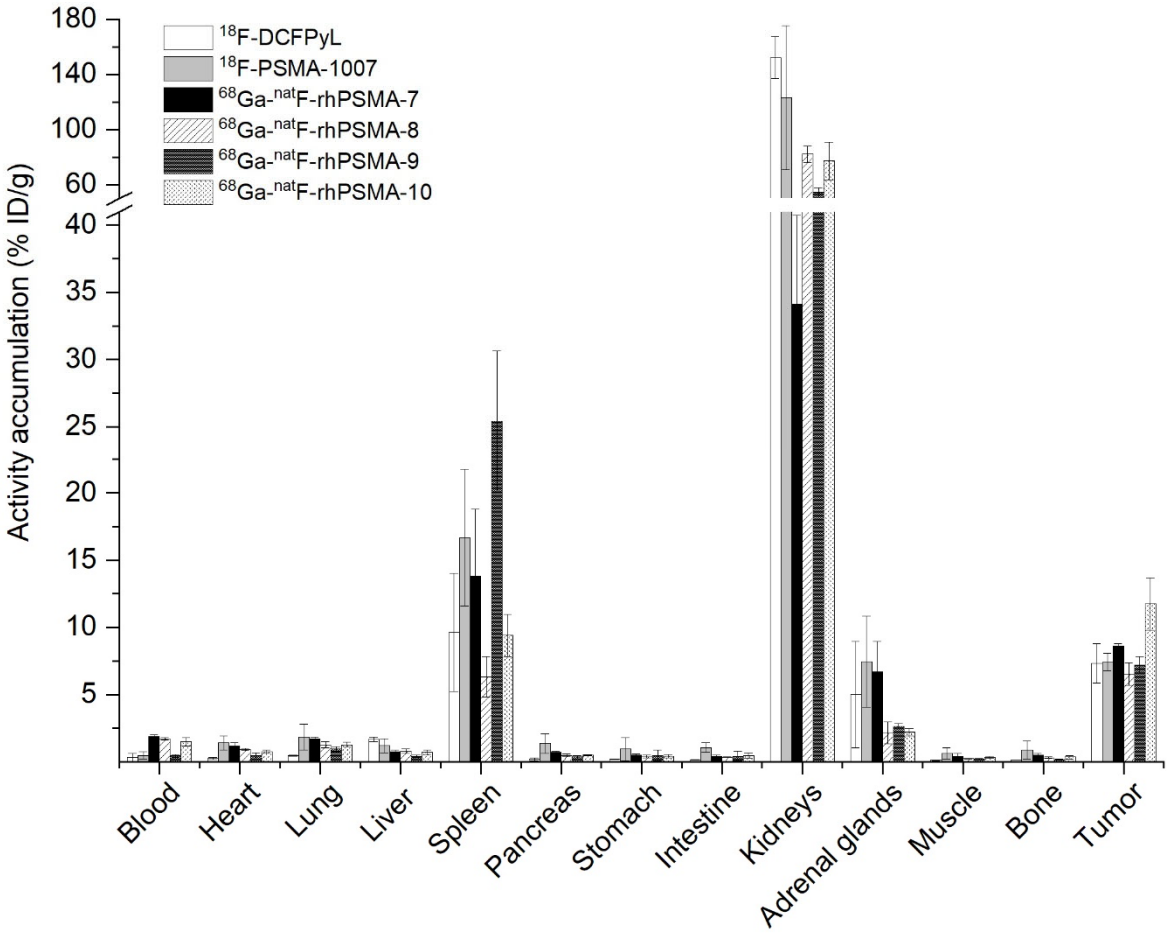

FIGURE 4. Biodistribution of ^{68}Ga-^{19}F-rhPSMA-7 to 10 and the reference ligands ^{18}F-DCFPyL and ^{18}F-PSMA-1007 at 1 h p.i. in LNCaP tumor-bearing SCID mice (n=3 for ^{68}Ga-^{19}F-rhPSMA-7 to 9, n=4 for ^{68}Ga-^{19}F-rhPSMA-10, ^{18}F-DCFPyL and ^{18}F-PSMA-1007). Data for reference ligands were taken from a previously published study by our group (*32*). Values are expressed as a percentage of injected dose per gram (%ID/g), mean ± standard deviation.

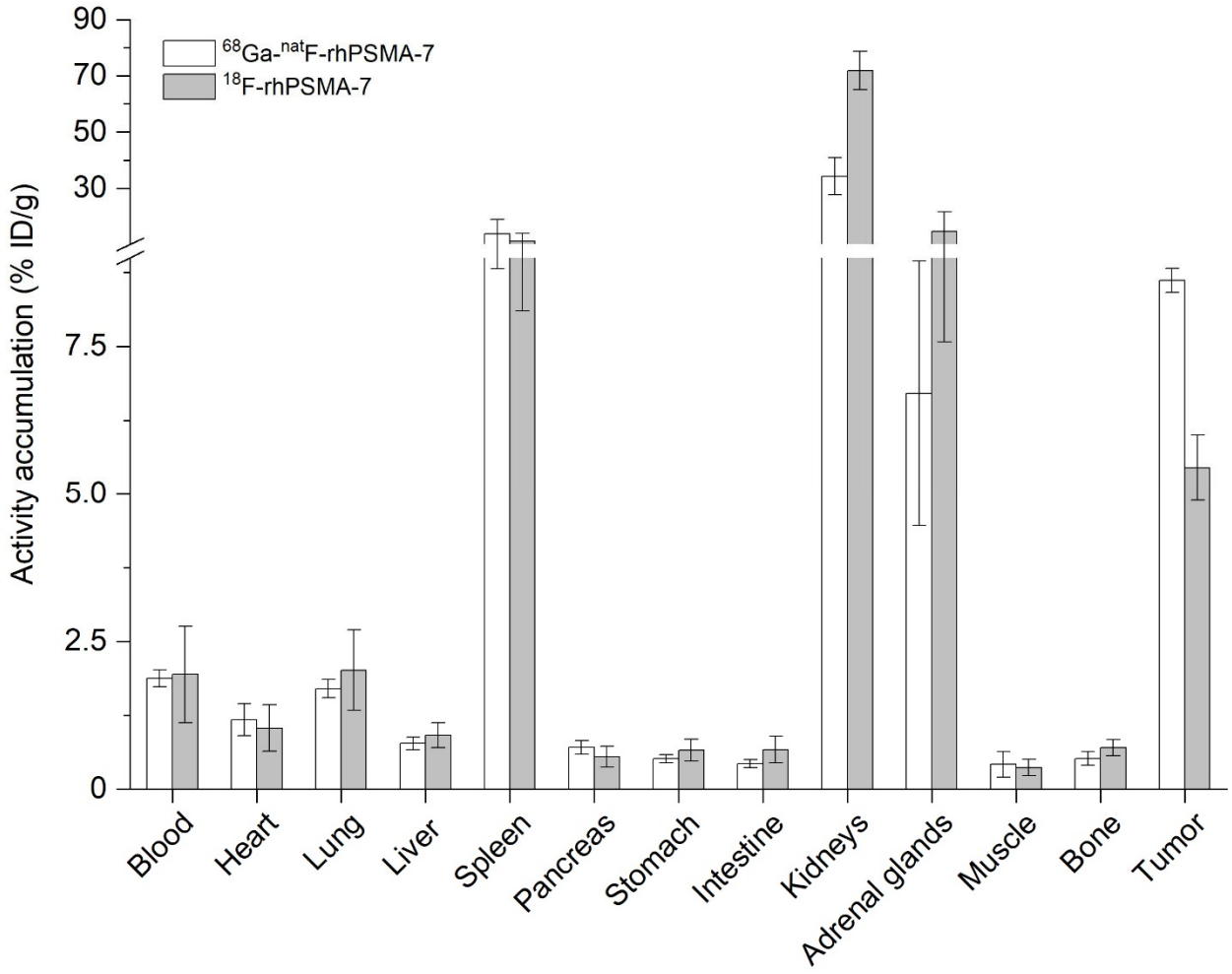

FIGURE 5. Comparative biodistribution of ^{68}Ga-^{19}F-rhPSMA-7 (white bars) and ^{18}F-rhPSMA-7 (grey bars) at 1 h p.i. in LNCaP tumor-bearing SCID mice (n=3). Data are expressed as a percentage of injected dose per gram (%ID/g) (mean ± standard deviation).

Radiohybrid ligands: a novel tracer concept exemplified by the development, radiolabeling and comparative preclinical evaluation of hybrid ^{18}F- or ^{68}Ga-labeled PSMA-inhibitors

- Supporting Information -

Alexander Wurzer[1], Daniel Di Carlo[1], Alexander Schmidt[1], Roswitha Beck[1], Matthias Eiber[2], Markus Schwaiger[2] and Hans-Jürgen Wester[1]

[1] Chair of Pharmaceutical Radiochemistry, Technical University of Munich, Garching, Germany;

[2] Department of Nuclear Medicine, Klinikum rechts der Isar, Technical University of Munich, Munich, Germany.

Corresponding author:

Hans-Jürgen Wester, PhD
Phone: +49.89.289.12203
Technical University of Munich,
Chair of Pharmaceutical Radiochemistry,
Walther-Meißner-Str. 3
85748 Garching
GERMANY
Fax: +49.89.289.12204
Email: H.J.Wester@tum.de

1. General Information

The Fmoc-(9-fluorenylmethoxycarbonyl-) and all other protected amino acid analogs were purchased from Bachem (Bubendorf, Switzerland) or Iris Biotech (Marktredwitz, Germany). The tritylchloride polystyrene (TCP) resin was obtained from PepChem (Tübingen, Germany). Chematech (Dijon, France) delivered the chelators DOTAGA (2-(4,7,10-tris(carboxymethyl)-1,4,7,10-tetraazacyclododecan-1-yl)pentanedioic acid), DOTA (1,4,7,10-Tetraazacyclododecane-1,4,7,10-tetraacetic acid), NOTA (2,2′,2”-(1,4,7-triazacyclononane-1,4,7-triyl)triacetic acid) and derivatives thereof. All necessary solvents and other organic reagents were purchased from either, Alfa Aesar (Karlsruhe, Germany), Sigma-Aldrich (Munich, Germany), Fluorochem (Hadfield, UK) or VWR (Darmstadt, Germany).

The *t*Bu-protected PSMA-addressing binding motifs, Lys-urea-Glu ((*t*BuO)KuE(O*t*Bu)$_2$) and Glu-urea-Glu ((tBuO)EuE(OtBu)$_2$) as well as the derivative PfpO-Sub-(*t*BuO)KuE(O*t*Bu)$_2$ (Pentafluorophenyl-suberic acid active ester of the *t*Bu-protected EuK binding motif) were prepared in analogy to previously described procedures (*1-3*). Synthesis of the Silicon-Fluoride-Acceptor, 4-(di-tert-butylfluorosilyl)benzoic acid (SiFA-BA) and the alkyne-functionalized TRAP chelator (1,4,7-triazacyclononane-1,4,7-tris[methyl(2-carboxyethyl)phosphinic acid) were performed according to the literature protocols (*4,5*).

Solid phase synthesis of the peptides was carried out by manual operation using an syringe shaker (Intelli, Neolab, Heidelberg, Germany). Analytical and preparative reversed-phase high-pressure liquid chromatography (RP-HPLC) were performed using Shimadzu gradient systems (Shimadzu, Neufahrn, Germany), each equipped with a SPD-20A UV/Vis detector (220 nm, 254 nm). A Nucleosil 100 C18 (125 × 4.6 mm, 5 µm particle size) column (CS Chromatographie Service, Langerwehe, Germany) was used for analytical measurements at a flow rate of 1 mL/min. Both specific gradients and the corresponding retention times t_R are cited in the text. Preparative HPLC purification was done with a Multospher 100 RP 18 (250 × 10 mm, 5 µm particle size) column (CS Chromatographie Service, Langerwehe, Germany) at a constant flow rate of 5 mL/min. Analytical and preparative radio RP-HPLC was performed using a Nucleosil 100 C18 (5 µm, 125 × 4.0 mm) column (CS Chromatographie Service, Langerwehe, Germany). Eluents for all HPLC operations were water (solvent A) and acetonitrile (solvent B), both containing 0.1%

trifluoroacetic acid. Radioactivity was detected through connection of the outlet of the UV-photometer to a HERM LB 500 NaI detector (Berthold Technologies, Bad Wildbad, Germany). Electrospray ionization-mass spectra for characterization of the substances were acquired on an expression^{L} CMS mass spectrometer (Advion, Harlow, United Kingdom). NMR spectra were recorded on Bruker (Billerica, USA) AVHD-300 or AVHD-400 spectrometers at 300 K. Activity quantification was performed using a 2480 WIZARD^{2} automatic gamma counter (PerkinElmer, Waltham, United States). Radio-thin layer chromatography (TLC) was carried out with a Scan-RAM detector (LabLogic Systems, Sheffield, United Kingdom).

2. General Procedures (GP) for peptide synthesis

TCP-resin loading (GP1)

Loading of the tritylchloride polystyrene (TCP) resin with a Fmoc-protected amino acid (AA) was carried out by stirring a solution of the TCP-resin (1.60 mmol/g) and Fmoc-AA-OH (1.5 eq.) in anhydrous DCM with DIPEA (3.8 eq.) at room temperature for 2 h. Remaining tritylchloride was capped by the addition of methanol (2 mL/g resin) for 15 min. Subsequently the resin was filtered and washed with DCM (2 × 5 mL/g resin), DMF (2 × 5 mL/g resin), methanol (5 mL/g resin) and dried *in vacuo*. Final loading *l* of Fmoc-AA-OH was determined by the following equation:

$$l\left[\frac{mmol}{g}\right] = \frac{(m_2 - m_1)\times 1000}{(M_W - M_{HCl})\, m_2}$$

m_2 = mass of loaded resin [g]
m_1 = mass of unloaded resin [g]
M_W = molecular weight of AA [g/mol]
M_{HCl} = molecular weight of HCl [g/mol]

On-resin Amide Bond Formation (GP2)

For conjugation of a building block to the resin-bound peptide, a mixture of TBTU with HOBt or HOAt is used for pre-activation of the carboxylic with DIPEA as a base in DMF (10 mL/g resin). After 5 min at rt,

the solution is added to the swollen resin. The exact stoichiometry and reaction time for each conjugation step is given in the respective synthesis protocols. After reaction, the resin was washed with DMF (6 × 5 mL/g resin).

On-resin Fmoc-deprotection (GP3)

The resin-bound Fmoc-peptide was treated with 20% piperidine in DMF (*v/v*, 8 mL/g resin) for 5 min and subsequently for 15 min. Afterwards, the resin was washed thoroughly with DMF (8 × 5 mL/g resin).

On-resin Dde-deprotection (GP4)

The Dde-protected peptide (1.0 eq.) was dissolved in a solution of 2% hydrazine monohydrate in DMF (*v/v*, 5 mL/g resin) and shaken for 20 min (GP4a). In the case of present Fmoc-groups, Dde-deprotection was performed by adding a solution of imidazole (0.92 g/g resin), hydroxylamine hydrochloride (1.26 g/g reisn) in NMP (5.0 mL/g resin) and DMF (1.0 mL/g resin) for 3 h at room temperature (GP4b). After deprotection the resin was washed with DMF (8 × 5 mL/g resin).

On-resin Allyl-deprotection (GP5)

The allyl-protecting group was removed by the addition of triisopropylsilane (TIPS) (50.0 eq.) and tetrakis(triphenylphosphine)palladium(0) ($Pd(PPh_3)_4$) (0.3 eq.) dissolved in DCM (8 mL/g resin). After 1.5 h at room temperature, the resin was washed with DCM (6 × 5 mL/g resin) and DMF (6 × 5 mL/g resin).

tBu/Boc deprotection (GP6)

Removal of *t*Bu/Boc-protecting groups was carried out by dissolving the crude product in a mixture of TFA/TIPS/water (*v/v/v*; 95/2.5/2.5) and stirring for 1-6 h at rt. Product formation was monitored by HPLC-analysis. After removing TFA under a stream of nitrogen, the residue was dissolved in a mixture of *tert*-butanol and water. After lyophilisation the crude peptide was obtained.

Peptide cleavage from the resin (GP7)

a. Preservation of acid labile protecting groups (GP7a): The resin-bound peptide was dissolved in a mixture of DCM/TFE/AcOH (*v/v/v*; 6/3/1, 8 mL/g resin) and shaken for 30 min. The solution containing the fully protected peptide was filtered off and the resin was treated with another portion of the cleavage solution for 30 min. Both fractions were combined and acetic acid was removed under reduced pressure by successively adding toluene and water. After lyophilisation of remaining water, the crude fully protected peptide was obtained.

b. Deprotection of all acid labile protecting groups (GP7b): The fully protected resin-bound peptide was dissolved in a mixture of TFA/TIPS/water (*v/v/v*; 95/2.5/2.5) and shaken for 30 min. The solution was filtered off and the resin was treated in the same way for another 30 min. Both filtrates were combined, stirred for additional 1-6 h at rt. Product formation was monitored by HPLC. After removing TFA under a stream of nitrogen, the residue was dissolved in a mixture of *tert*-butanol and water and freeze-dried.

Conjugation of PfpO-Sub-(tBuO)KuE(OtBu)$_2$ to the peptide (GP8)

The *N*-terminal deprotected peptide (1.0 eq.) was added to a solution of **3** (1.2 eq.) in DMF (approx. 0.1 mL/ mg peptide) and TEA (8 eq.) was added. After stirring the solution for 2 h at rt, DMF was removed *in vacuo*. For cleavage of the *t*Bu-esters, TFA was added and the solution was stirred for 45 min at rt. After removing TFA under a stream of nitrogen, the crude product was purified by RP-HPLC.

Coupling of propargyl-TRAP to the peptide (GP9)

For conjugation of azide-functionalized peptides to propargyl-TRAP via copper(I)-catalyzed alkyne-azide cycloaddition a previously developed procedure was applied (*5*). Briefly, propargyl-TRAP (1.0 eq.) was dissolved in water (40 mM solution) and combined with a solution of the peptide (1.1 eq.) in a 1:1 (*v/v*) mixture of *t*BuOH and water (approx. 20-40 mM). Subsequently, a solution of sodium ascorbate (0.5 M,

50 eq.) in water was added. In order to start the reaction, an aqueous solution of $Cu(OAc)_2 \cdot H_2O$ (0.05 M, 1.2 eq.) was added, which resulted in a brown precipitate that dissolved after stirring in a clear green solution. For demetallation of TRAP, an aqueous solution of NOTA (8 mM, 12 eq.) was added and the pH was adjusted to 2.2 with 1 M aq. HCl. After either 1 h at 60 °C, or 48 h at rt the mixture was directly subjected to preparative HPLC purification.

Conjugation of DOTAGA anhydride (GP10)

The *N*-terminal deprotected peptide (1.0 eq.) was dissolved together with DOTAGA-anhydride (1.5 eq.) and DIPEA (10.0 eq.) in dry DMF. After stirring the reaction mixture overnight at rt, DMF was removed *in vacuo*, yielding the crude product.

3. Synthesis of rhPSMA ligands

rhPSMA-5

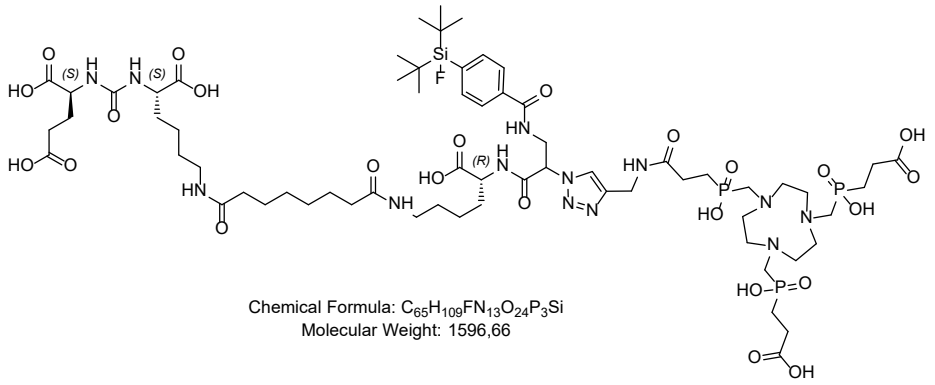

Supplemental Figure 1. Structural formula of uncomplexed rhPSMA-5.

Synthesis of rhPSMA-5 was carried out by applying the general methods and procedures mentioned before. Shortly, resin-bound Fmoc-D-Lys(Boc)-OH was Fmoc-deprotected with 20% piperidine in DMF (GP3) and conjugated to N_3-L-Dap(Fmoc)-OH (2.0 eq.) with HATU (3.0 eq.), HOAt (3.0 eq.) and DIPEA (6.0 eq.) for 2 h in DMF (GP2). After cleavage of the Fmoc-group (GP3), SiFA-BA (1.5 eq.) was added with HOBt

(1.5 eq.), TBTU (1.5 eq.) and DIPEA (4.5 eq.) in DMF for 2 h (GP2). Subsequent cleavage from the resin with TFA yielded the fully deprotected peptide backbone (GP7b). For conjugation of the EuK-moiety, PfpO-Sub-(*t*BuO)KuE(O*t*Bu)$_2$ (1.2 eq.) was added in a mixture of TEA (8 eq.) and DMF (GP8). Cleavage of the *t*Bu-esters was performed by adding TFA (GP6). In a final step the purified peptide (1.1 eq.) was reacted with propargyl-TRAP (1.0 eq.) in a *copper(I)-catalyzed* click reaction, as mentioned above (GP9). After RP-HPLC purification rhPSMA-5 (4%) was obtained as a colourless solid. HPLC (10 to 90% B in 15 min): t_R = 8.5 min. Calculated monoisotopic mass ($C_{65}H_{109}FN_{13}O_{24}P_3Si$): 1595.7; found: m/z = 1596.5 $[M+H]^+$, 799.1 $[M+2H]^{2+}$.

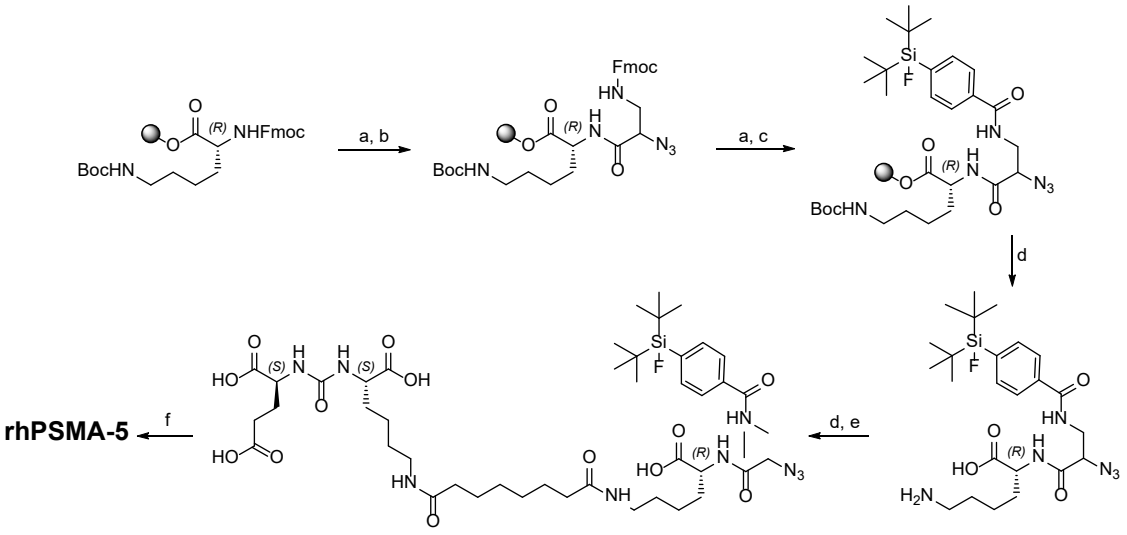

Supplemental Figure 2. Synthesis of rhPSMA-5: a) 20% piperidine (DMF); b) N_3-L-Dap(Fmoc)-OH, HATU, HOAt, DIPEA (DMF); c) SIFA-BA, HOBt, TBTU, DIPEA (DMF); d) TFA; e) PfpO-Sub-(*t*BuO)-KuE(O*t*Bu)$_2$, TEA (DMF); f) propargyl-TRAP, $Cu(OAc)_2 \cdot H_2O$, sodium ascorbate (*t*BuOH, H_2O).

rhPSMA-6

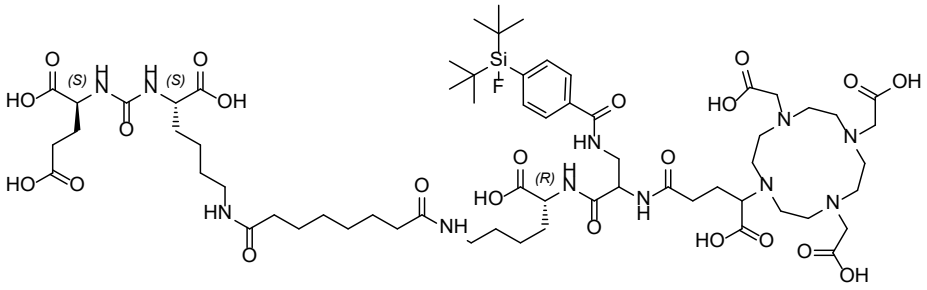

Supplemental Figure 3. Structural formula of uncomplexed rhPSMA-6.

Resin-bound Fmoc-D-Lys(Boc) was Fmoc deprotected with 20% piperidine in DMF (GP3) and Fmoc-D-Dap(Dde)-OH (2.0 eq.) was conjugated applying HOBt (2.0 eq.), TBTU (2.0 eq.) and DIPEA (6.0 eq.) in DMF for 2 h (GP2). After orthogonal Dde-deprotection with imidazole and hydroxylamine hydrochloride in a mixture of NMP and DMF (GP4b), SIFA-BA (1.5 eq.) was conjugated with HOBt (1.5 eq.), TBTU (1.5 eq.) and DIPEA (4.5 eq.) in DMF for 2 h (GP2). Subsequent Fmoc-deprotection (GP3) and mild cleavage from the resin with TFE and AcOH in DCM (GP7a) yielded the *t*Bu-protected peptide backbone. Condensation of DOTAGA-anhydride (1.5 eq.) was performed by adding DIPEA (10 eq.) in DMF (GP10). After *t*Bu-deprotection in TFA (GP6), the PfpO-Sub-(tBuO)KuE(OtBu)$_2$ moiety (1.2 eq.) was added in a mixture of TEA (8 eq.) and DMF (GP8). Final cleavage of the *t*Bu-esters in TFA (GP6) and RP-HPLC purification yielded rhPSMA-6 (70%) as a colorless solid. HPLC (10 to 90% B in 15 min): t_R = 9.1 min. Calculated monoisotopic mass ($C_{63}H_{102}FN_{11}O_{22}Si$): 1411.7; found: m/z = 1412.3 $[M+H]^+$, 706.8 $[M+2H]^{2+}$.

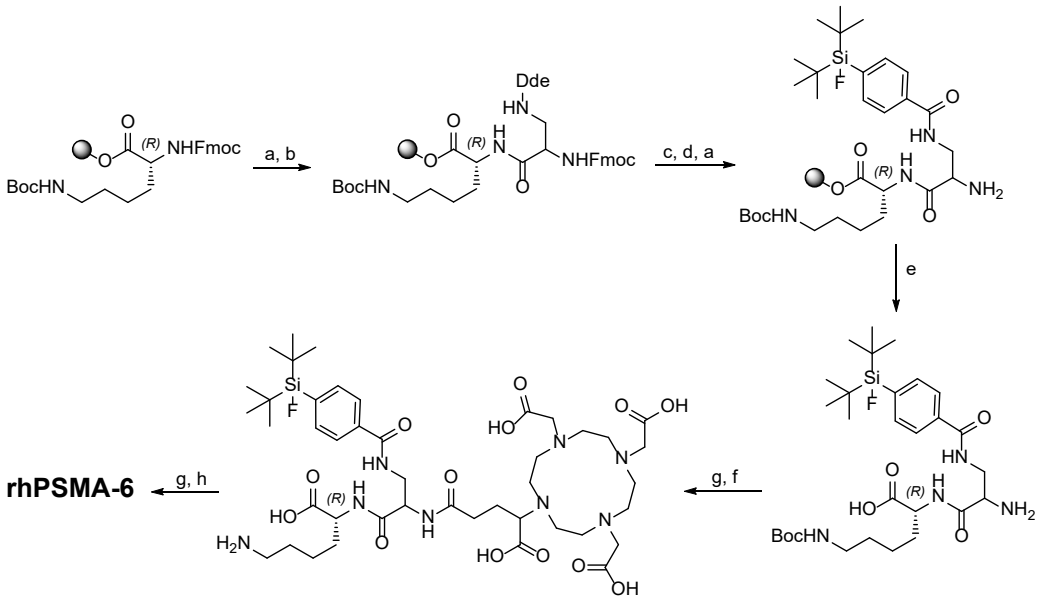

Supplemental Figure 4. Synthesis of rhPSMA-6: a) 20% piperidine (DMF); b) Fmoc-D-Dap(Dde)-OH, HOBt, TBTU, DIPEA (DMF); c) imidazole, hydroxylamine hydrochloride (NMP, DMF); d) SIFA-BA, HOBt, TBTU, DIPEA (DMF); e) TFE, AcOH (DCM); f) DOTAGA-anhydride, DIPEA (DMF); g) TFA; h) PfpO-Sub-(*t*BuO)KuE(O*t*Bu)$_2$, TEA (DMF).

rhPSMA-7

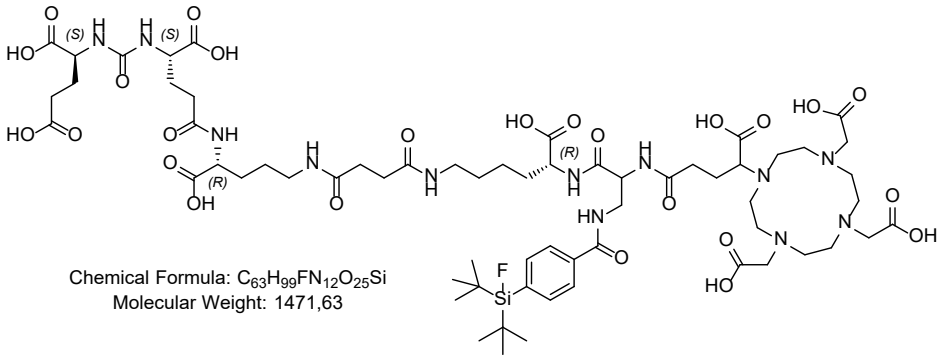

Supplemental Figure 5. Structural formula of uncomplexed rhPSMA-7.

Resin-bound Fmoc-D-Orn(Dde)-OH was Fmoc-deprotected with 20% piperidine in DMF (GP3) and (*t*BuO)EuE(O*t*Bu)$_2$ (2.0 eq.) was conjugated with HOBt (2.0 eq.), TBTU (2.0 eq.) and DIPEA (6.0 eq.) in DMF for 4.5 h (GP3). After cleavage of the Dde-group with a mixture of 2% hydrazine in DMF (GP4a), a solution of succinic anhydride (7.0 eq.) and DIPEA (7.0 eq.) in DMF was added and reacted for 2.5 h. Conjugation of Fmoc-D-Lys-OAll·HCl (1.5 eq.) was achieved by adding a mixture of HOBt (1.5 eq.), TBTU (1.5 eq.) and DIPEA (4.5 eq.) in DMF for 2 h (GP2). After cleavage of the Fmoc-group with 20% piperidine in DMF (GP3), the free amine was conjugated to Fmoc-D-Dap(Dde)-OH (2.0 eq.) after pre-activation of the amino acid in a mixture of HOBt (2.0 eq.), TBTU (2.0 eq.) and DIPEA (6.0 eq.) in DMF for 2 h (GP2). Following orthogonal Dde-deprotection was done using imidazole and hydroxylamine hydrochloride dissolved in a mixture of NMP and DMF (GP4b). SiFA-BA (1.5 eq.) was reacted with the free amine of the side chain with HOBt (1.5 eq.), TBTU (1.5 eq.) and DIPEA (4.5 eq.) as activation reagents in DMF for 2 h (GP2). The allyl-protecting group was removed by the addition of TIPS (50.0 eq.) and Pd(PPh$_3$)$_4$ (0.3 eq.) dissolved in DCM (GP5). After Fmoc-deprotection with piperidine (GP3), the peptide was cleaved from the resin under preservation of the acid labile protecting groups by using a mixture of TFE and AcOH in DCM (GP7a). Final condensation of DOTAGA-anhydride (1.5 eq.) was achieved with piperidine (10 eq.) in DMF (GP10). After cleavage of the *t*Bu-esters of the EuE-moiety with TFA (GP6), the crude peptide was purified by RP-HPLC, yielding rhPSMA-7 (24%) as a colorless solid. HPLC (10 to 70% B in 15 min): t_R = 10.4 min. Calculated monoisotopic mass ($C_{63}H_{99}FN_{12}O_{25}Si$): 1470.7; found: m/z = 1471.8 $[M+H]^+$, 736.7 $[M+2H]^{2+}$.

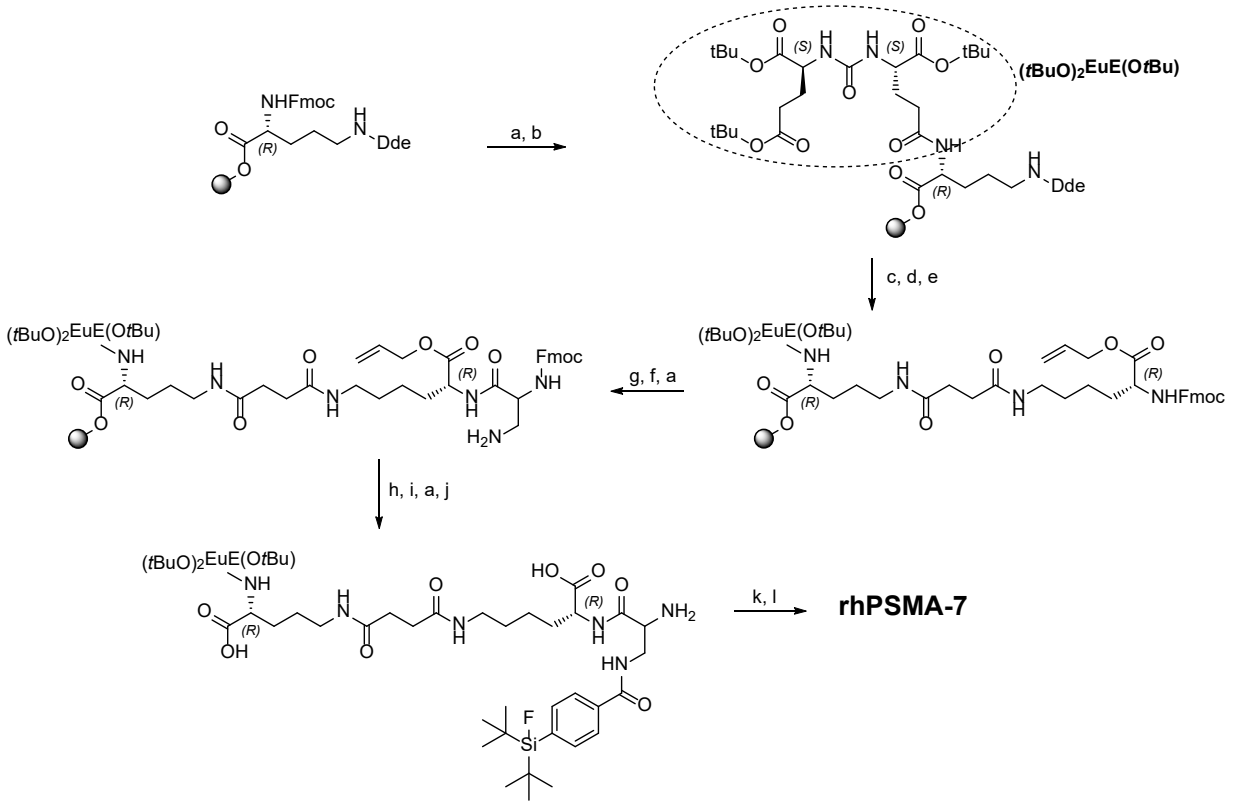

Supplemental Figure 6. Synthesis of rhPSMA-7: a) 20% piperidine (DMF); b) (tBuO)EuE(OtBu)$_2$, HOBt, TBTU, DIPEA (DMF); c) 2% hydrazine (DMF); d) succinic anhydride, DIPEA (DMF); e) Fmoc-D-Lys-OAll·HCl, HOBt, TBTU, DIPEA (DMF); f) Fmoc-D-Dap(Dde)-OH, HOBt, TBTU, DIPEA (DMF); g) imidazole, hydroxylamine hydrochloride (NMP, DMF); h) SiFA-BA, HOBt, TBTU, DIPEA (DMF); i) TIPS, Pd(PPh$_3$)$_4$ (DCM); j) TFE, AcOH (DCM); k) DOTAGA-anhydride, DIPEA (DMF); l) TFA.

rhPSMA-8

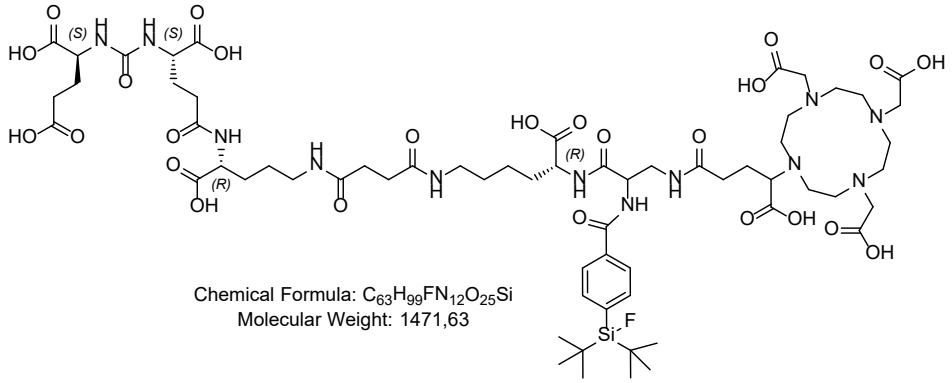

Supplemental Figure 7. Structural formula of uncomplexed rhPSMA-8.

Synthesis of rhPSMA-8, was carried out as described for rhPSMA-7, with one deviation; After conjugation of Fmoc-D-Dap(Dde)-OH, the Fmoc-protecting group was cleaved with piperidine in DMF (GP3) and SiFA-BA was reacted with the free N-terminus of the peptide (GP2). After removing the allyl-protecting group with TIPS (50.0 eq.) and $Pd(PPh_3)_4$ (0.3 eq.) dissolved in DCM (GP5), the remaining Dde-group was cleaved by a solution of imidazole and hydroxylamine hydrochloride dissolved in NMP and DMF (GP4b). Following conjugation of DOTAGA and final deprotection were carried out as described for rhPSMA-7. After RP-HPLC purification, rhPSMA-8 (11%) was obtained as a colorless solid. HPLC (10 to 70% B in 15 min): t_R = 10.4 min. Calculated monoisotopic mass ($C_{63}H_{99}FN_{12}O_{25}Si$): 1470.7; found: m/z = 1471.7 $[M+H]^+$, 736.8 $[M+2H]^{2+}$.

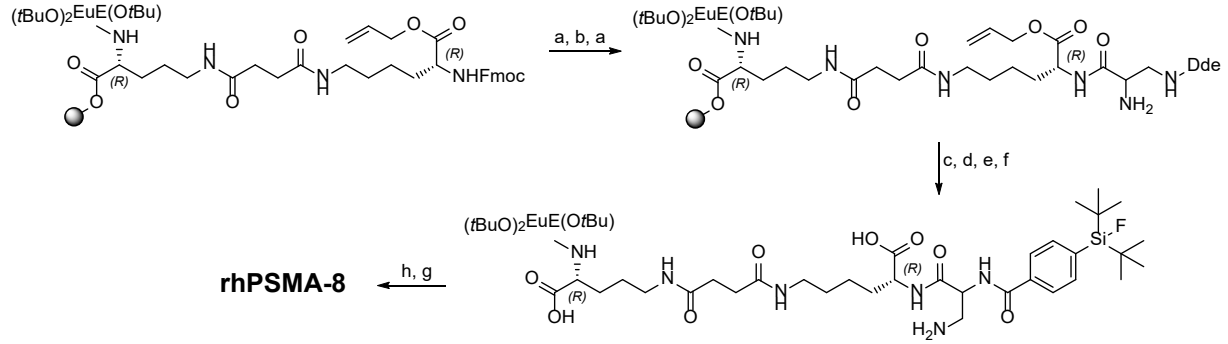

Supplemental Figure 8. Synthesis of rhPSMA-8: a) 20% piperidine (DMF); b) Fmoc-D-Dap(Dde)-OH, HOBt, TBTU, DIPEA (DMF); c) SIFA-BA, HOBt, TBTU, DIPEA (DMF); d) TIPS, $Pd(PPh_3)_4$ (DCM); e) imidazole, hydroxylamine hydrochloride (NMP, DMF); f) TFE, AcOH (DCM); g) DOTAGA-anhydride, DIPEA (DMF); h) TFA.

rhPSMA-9

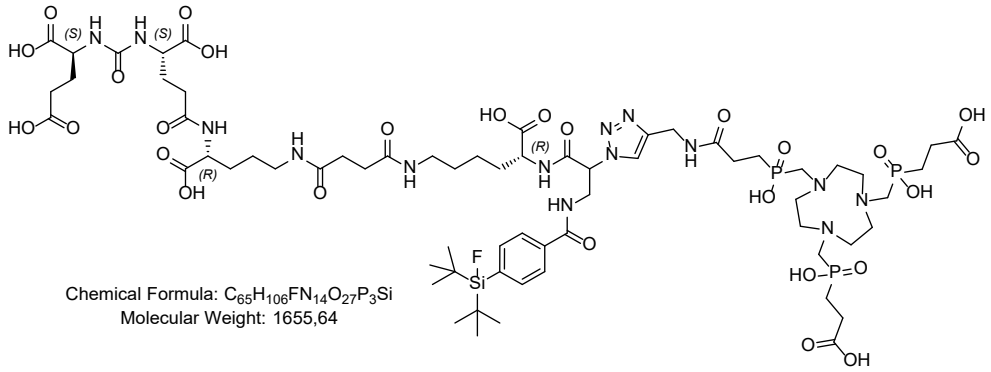

Supplemental Figure 9. Structural formula of uncomplexed rhPSMA-9.

The peptide backbone of rhPSMA-9 was prepared analogously to rhPSMA-7 and 8. A difference was the use of N_3-L-Dap(Fmoc)-OH instead of Fmoc-D-Dap(Dde)-OH, which was required for the final click reaction with propargyl-TRAP. The azido-substituted amino acid (2.0 eq.) was conjugated with HATU (3.0 eq.), HOAt (3.0 eq.) and DIPEA (6.0 eq.) in DMF for 2 h (GP2). After Fmoc-deprotection with 20% piperidine (GP3), SIFA-BA (1.5 eq.) was reacted with HOBt (1.5 eq.), TBTU (1.5 eq.) and DIPEA (4.5 eq.) as activation reagents in DMF for 2 h (GP2). Removal of the allyl-protecting group was performed by the addition of TIPS (50.0 eq.) and $Pd(PPh_3)_4$ (0.3 eq.) dissolved in DCM (GP5). After cleavage from the resin with TFA under concurrent deprotection of all acid labile protecting groups (GP7b), the purified EuE-azido-conjugate (1.1 eq.) was reacted with propargyl-TRAP (1.0 eq.) in a copper(I)-catalyzed click reaction (GP9). RP-HPLC purification yielded rhPSMA-9 (9%) as a colourless solid. HPLC (10 to 90% B in 15 min): t_R = 8.7 min. Calculated monoisotopic mass ($C_{65}H_{106}FN_{14}O_{27}P_3Si$): 1654.6; found: m/z = 1655.6 $[M+H]^+$, 828.4 $[M+2H]^{2+}$.

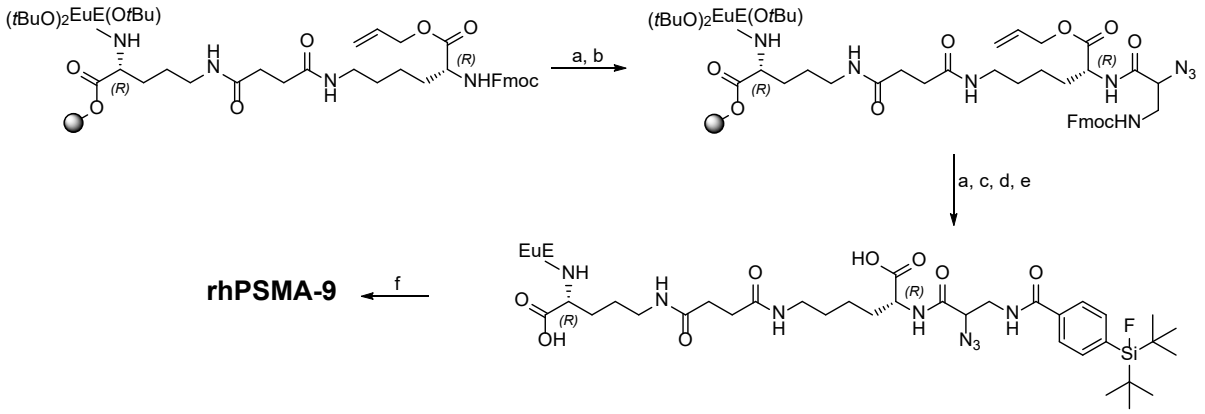

Supplemental Figure 10. Synthesis of rhPSMA-9: a) 20% piperidine (DMF); b) N_3-L-Dap(Fmoc)-OH, HOBt, TBTU, DIPEA (DMF); c) SIFA-BA, HOBt, TBTU, DIPEA (DMF); d) TIPS, $Pd(PPh_3)_4$ (DCM); e) TFA; f) propargyl-TRAP, $Cu(OAc)_2 \cdot H_2O$, sodium ascorbate (*t*BuOH, H_2O).

rhPSMA-10

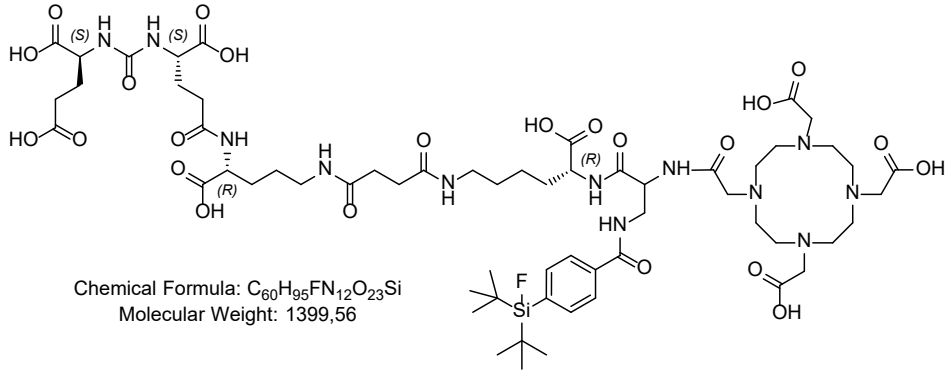

Supplemental Figure 11. Structural formula of uncomplexed rhPSMA-10.

rhPSMA-10 was synthesized in analogy to rhPSMA-7, by using DOTA instead of DOTAGA, starting from resin-bound ((*t*Bu$_2$)EuE(*t*Bu)-orn-succinic acid. Conjugation of Fmoc-D-Lys(O*t*Bu)·HCl (1.5 eq.) was achieved by adding a mixture of HOBt (1.5 eq.), TBTU (1.5 eq.) and DIPEA (4.5 eq.) in DMF for 2 h (GP2). After cleavage of the Fmoc-group (GP3), Fmoc-D-Dap(Dde)-OH (2.0 eq.) was pre-activated in a mixture of HOAt (2.0 eq.), TBTU (2.0 eq.) and DIPEA (6.0 eq.) in DMF and added to the resin-bound peptide for 2.5 h (GP2). Following orthogonal Dde-deprotection was done using imidazole and hydroxylamine hydrochloride dissolved in a mixture of NMP and DMF for 3 h (GP4b). SiFA-BA (1.5 eq.) was reacted with

the free amine of the side chain with HOAt (1.5 eq.), TBTU (1.5 eq.) and DIPEA (4.5 eq.), as activation reagents in DMF for 2 h (GP2). After Fmoc-deprotection with piperidine (GP3), the *tert*-butyl protected chelator, DOTA(tBu)$_3$ was conjugated with HOAt (2.0 eq.), TBTU (2.0 eq.) and DIPEA (6.0 eq.) in DMF for 2.5 h (GP2). Cleavage from the resin with simultaneous deprotection of acid labile protecting groups was performed in TFA for 6 h (GP7b). After HPLC-based purification, rhPSMA-10 (11%) was obtained as a colorless solid. HPLC (10 to 70% B in 15 min): t_R = 10.5 min. Calculated monoisotopic mass ($C_{60}H_{95}FN_{12}O_{23}Si$): 1398.6; found: m/z = 1399.6 $[M+H]^+$, 700.6 $[M+2H]^{2+}$.

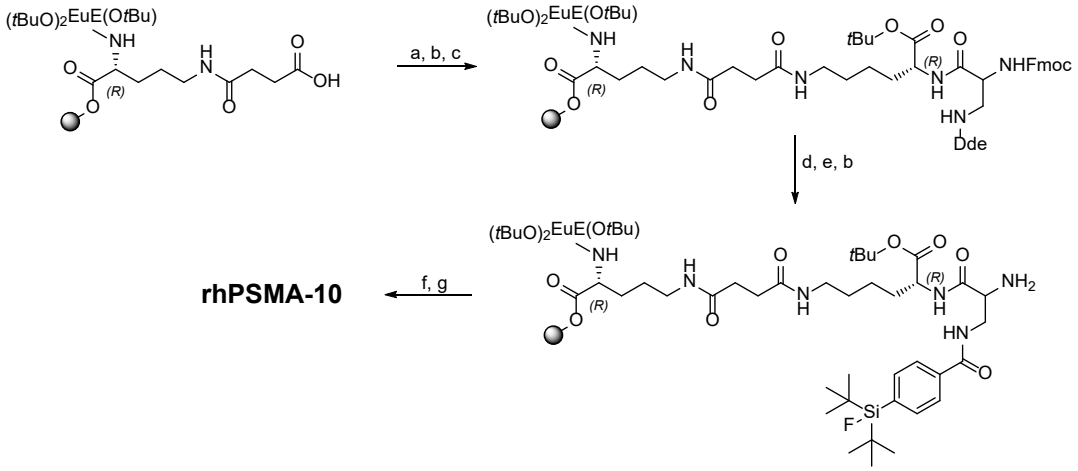

Supplemental Figure 12. Synthesis of rhPSMA-10: a) Fmoc-D-Lys(OtBu)·HCl, HOBt, TBTU, DIPEA (DMF) b) 20% piperidine (DMF); c) Fmoc-D-Dap(Dde)-OH, HOBt, TBTU, DIPEA (DMF); d) imidazole, hydroxylamine hydrochloride (NMP, DMF); e) SiFA-BA, HOBt, TBTU, DIPEA (DMF); f) DOTA(tBu)$_3$, HOBt, TBTU, DIPEA (DMF); g) TFA.

4. Synthesis of cold Gallium complexes

Synthesis of ^{nat}Ga-TRAP complexes

500 µL of a 2 mM stock solution of the rhPSMA precursor (1.0 eq.) in DMSO was combined with 75 µL of a 20 mM $Ga(NO_3)_3$ (1.5 eq.) solution in water. Complexation occurred instantaneously at room temperature. If required, purification of the crude ligand was performed by RP-HPLC.

^{nat}Ga-rhPSMA-5: *HPLC* (10 to 90% B in 15 min): t_R = 9.5 min. Calculated monoisotopic mass ($C_{65}H_{106}FGaN_{13}O_{24}P_3Si$): 1661.6; found: m/z = 1663.9 $[M+H]^+$, 832.6 $[M+2H]^{2+}$.

^{nat}Ga-rhPSMA-9: *HPLC* (10 to 90% B in 15 min): t_R = 9.0 min. Calculated monoisotopic mass ($C_{65}H_{103}FGaN_{14}O_{27}P_3Si$): 1720.5; found: m/z = 1720.8 $[M+H]^+$, 861.1 $[M+2H]^{2+}$.

Synthesis of ^{nat}Ga-DOTAGA and ^{nat}Ga-DOTA complexes

500 µL of a 2 mM stock solution of the rhPSMA precursor (1.0 eq.) in DMSO was combined with 150 µL of a 20 mM $Ga(NO_3)_3$ solution (3.0 eq.) in water. The reaction mixture was heated for 30 min at 75 °C. If required, the complexed compound was purified by RP-HPLC.

^{nat}Ga-rhPSMA-6: HPLC (10 to 90% B in 15 min): t_R = 9.1 min. Calculated monoisotopic mass ($C_{63}H_{99}FGaN_{11}O_{22}Si$): 1477.6; found: m/z = 1479.5 $[M+H]^+$, 740.2 $[M+2H]^{2+}$.

^{nat}Ga-rhPSMA-7: HPLC (10 to 70% B in 15 min): t_R = 10.4 min. Calculated monoisotopic mass ($C_{63}H_{96}FGaN_{12}O_{25}Si$): 1536.6; found: m/z = 1539.4 $[M+H]^+$, 770.3 $[M+2H]^{2+}$.

^{nat}Ga-rhPSMA-8: HPLC (10 to 70% B in 15 min): t_R = 10.4 min. Calculated monoisotopic mass ($C_{63}H_{96}FGaN_{12}O_{25}Si$): 1536.6; found: m/z = 1539.1 $[M+H]^+$, 770.5 $[M+2H]^{2+}$.

^{nat}Ga-rhPSMA-10: HPLC (10 to 70% B in 15 min): 9.5 min. Calculated monoisotopic mass ($C_{60}H_{92}FGaN_{12}O_{23}Si$): 1464.5; found: m/z = 1467.3 $[M+H]^+$, 733.9 $[M+2H]^{2+}$.

5. Radiolabelling

^{68}Ga-labelling was performed using an automated system (GallElut$^+$ by Scintomics, Germany) as described previously (*6*). Briefly, the ^{68}Ge/^{68}Ga-generator with SnO_2 matrix (IThemba LABS) was eluted with 1.0 M aqueous HCl, from which a fraction (1.25 mL) of approximately 80% of the activity (500–700 MBq), was transferred into a reaction vial (ALLTECH, 5 mL). The reactor was loaded before elution with 2–5 nmol of respective chelator conjugate in an aqueous 2.7 M HEPES solution (DOTA/DOTAGA-conjugates: 900 µL, TRAP-conjugates: 400 µL). After elution the vial was heated for 5 minutes at 95 °C. Purification was done by passing the reaction mixture over a solid phase extraction cartridge (C 8 light, SepPak), which was purged

with water (10 mL). The purified product was eluted with 50% aqueous ethanol (2 mL), phosphate buffered saline (PBS, 1 mL) and again water (1 mL). After removing ethanol *in vacuo*, purity of the radiolabelled compounds was determined by radio-HPLC and radio-TLC (ITLC-SG chromatography paper, mobile phase: 0.1 M trisodium citrate and Silica gel 60 RP-18 F_{254}s, mobile phase: 3:2 mixture (v/v) of MeCN in H_2O supplemented with 10% of 2 M NaOAc solution and 1% of TFA).

6. Human Serum Albumin (HSA) Binding

HSA binding of the PSMA-addressing ligands was determined according to a previously published procedure via HPLC (*7*). A Chiralpak HSA column (50 x 3 mm, 5 µm, H13H-2433, Daicel, Tokyo, Japan) was used at a constant flow rate of 0.5 mL/min at rt. Mobile phase A was a freshly prepared 50 mM aqueous solution of NH_4OAc (pH 6.9) and mobile phase B was isopropanol (HPLC grade, VWR, Germany). The applied gradient for all experiments was 100% A (0 to 3 min), followed by 80% A (3 to 40 min). Prior to the experiment, the column was calibrated using nine reference substances with a HSA binding, known from literature, in the range of 13 to 99% (*7,8*). All substances, including the examined PSMA ligands, were dissolved in a 1:1 mixture (v/v) of isopropanol and a 50 mM aqueous solution of NH_4OAc (pH 6.9) with a final concentration of 0.5 mg/mL. Non-linear regression was established with the OriginPro 2016G software (Northampton, United States).

7. *In vitro* Experiments

Affinity determinations (IC_{50})

The PSMA affinity (IC_{50}) determinations and synthesis of the radioiodinated reference ligand (((S)-1-carboxy-5-(4-^{125}I-iodobenzamido)pentyl)carbamoyl)-*L*-glutamic acid, (((^{125}I-I-BA)KuE) were performed as described previously (*1*). Briefly, the respective ligand was diluted (serial dilution 10^{-4} to 10^{-10}) in Hank's balanced salt solution (HBSS, Biochrom). In the case of metal-complexed ligands, the crude reaction mixture containing the purified metal-complexed inhibitor and remaining metal nitrate, was diluted

analogously without further purification.. Cells were harvested 24 ± 2 hours prior to the experiment and seeded in 24-well plates (1.5×10^5 cells in 1 mL/well). After removal of the culture medium, the cells were carefully washed with 500 µL of HBSS, supplemented with 1% bovine serum albumin (BSA, Biowest, Nuaillé, France) and left 15 min on ice for equilibration in 200 µL HBSS (1% BSA). Next, 25 µL per well of solutions, containing either HBSS (1% BSA, control) or the respective ligand in increasing concentration (10^{-10} – 10^{-4} M in HBSS) were added with subsequent addition of 25 µL of ^{125}I-I-BA-KuE (2.0 nM) in HBSS (1% BSA). After incubation on ice for 60 min, the experiment was terminated by removal of the medium and consecutive rinsing with 200 µL of HBSS (1% BSA). The media of both steps were combined in one fraction and represent the amount of free radioligand. Afterwards, the cells were lysed with 250 µL of 1 M aqueous NaOH for at least 10 min. After a washing step (250 µL of 1 M NaOH), both fractions, representing the amount of bound ligand, were united. Quantification of all collected fractions was accomplished in a γ-counter. PSMA-affinity determinations were carried out at least three times per ligand.

Internalization studies

Internalization studies were carried out according to a previously published procedure (*1*). Briefly, LNCaP cells were harvested 24 ± 2 hours before the experiment and seeded in poly-*L*-lysine coated 24-well plates (1.25×10^5 cells in 1 mL/well, Greiner Bio-One, Kremsmünster, Austria). After removal of the culture medium, the cells were washed once with 500 µL DMEM-F12 (5% BSA) and left to equilibrate for at least 15 min at 37 °C in 200 µL DMEM-F12 (5% BSA). Each well was treated with either 25 µL of either DMEM-F12 (5% BSA, control) or 25 µL of a 100 µM PMPA (2-(Phosphonomethyl)-pentandioic acid, Tocris Bioscience, Bristol, UK) solution in PBS, for blockade. Next, 25 µL of the radioactive-labelled PSMA inhibitor (5.0 nM in PBS) was added and the cells were incubated at 37 °C for 60 min. The experiment was terminated by placing the 24-well plate on ice for 3 min and consecutive removal of the medium. Each well was carefully washed with 250 µL of ice-cold HBSS. Both fractions from the first steps, representing the amount of free radioligand, were combined. Removal of surface bound activity was accomplished by incubation of the cells with 250 µL of ice-cold PMPA (10 µM in PBS) solution for 5 min

and rinsed again with another 250 µL of ice-cold PBS. The internalized activity was determined by incubation of the cells in 250 µL 1 M aqueous NaOH for at least 10 min. The obtained fractions were combined with those of the subsequent wash step with 250 µL 1 M aqueous NaOH. Each experiment (control and blockade) was performed in triplicate. Free, surface bound and internalized activity was quantified in a γ-counter. All internalization studies were accompanied by external reference studies, using (^{125}I-I-BA)KuE (0.2 nM/well), which were performed analogously. Data were corrected for non-specific binding and normalized to the specific-internalization observed for the radioiodinated reference compound.

8. Supplemental Data 1

Supplemental Table 1. Binding affinities (IC_{50} in nM, 1 h, 4°C; n=3) of ^{nat}Ga-^{19}F-rhPSMA-5–10, ^{19}F-rhPSMA-5–10 with free chelator, ^{19}F-DCFPyL and ^{19}F-PSMA-1007; internalized activity of ^{18}F-DCFPyL, ^{18}F-PSMA-1007, ^{68}Ga-^{19}F-rhPSMA-5–10 and ^{18}F-rhPSMA-5–10 with free chelator in LNCaP cells (1 h, 37°C) as percent of the reference ligand (^{125}I-I-BA)KuE; n=3); lipophilicity of ^{18}F-DCFPyL, ^{18}F-PSMA-1007, ^{68}Ga-^{19}F-rhPSMA-5–10 and ^{18}F-rhPSMA-5–10 with free chelator, expressed as octanol/PBS (pH 7.4) partition-coefficient (log $P_{oct/PBS}$; n=6); HSA binding of ^{19}F-DCFPyL, ^{19}F-PSMA-1007, ^{nat}Ga-^{19}F-rhPSMA-5–10, determined on a Chiralpak HSA column. Data of reference ligands $^{18/19}$F-DCFPyL and $^{18/19}$F-PSMA-1007 from a previously published study (*3*). Values are expressed as mean ± standard deviation.

Ligand	IC_{50} [nM]	Internalization [% of reference]	Lipophilicity log $P_{O/PBS}$	HSA-binding [%]
$^{68/nat}$Ga-$^{19/18}$F-rhPSMA-5	10.8 ± 2.5	43 ± 3	- 3.0 ± 0.09	-
$^{19/18}$F-rhPSMA-5	8.5 ± 1.7	-	-	
$^{68/nat}$Ga-$^{19/18}$F-rhPSMA-6	7.3 ± 0.2	33 ± 2	- 2.8 ± 0.07	-
$^{19/18}$F-rhPSMA-6	6.4 ± 0.2	-	-	
$^{68/nat}$Ga-$^{19/18}$F-rhPSMA-7	3.0 ± 0.7	126 ± 13	- 3.2 ± 0.05	96
$^{19/18}$F-rhPSMA-7	3.5 ± 0.2	165 ± 5	- 2.0 ± 0.04	-
$^{68/nat}$Ga-$^{19/18}$F-rhPSMA-8	3.8 ± 0.7	98 ± 12	- 2.6 ± 0.04	97
$^{19/18}$F-rhPSMA-8	2.5 ± 0.2	130 ± 6	- 2.3 ± 0.07	-
$^{68/nat}$Ga-$^{19/18}$F-rhPSMA-9	4.5 ± 0.3	180 ± 12	- 3.3 ± 0.06	95
$^{19/18}$F-rhPSMA-9	4.3 ± 0.2	212 ± 5	- 2.2 ± 0.07	-
$^{68/nat}$Ga-^{19}F-rhPSMA-10	3.8 ± 0.3	131 ± 14	- 3.5 ± 0.07	94
$^{19/18}$F-DCFPyL	12.3 ± 1.2	118 ± 4	- 3.4 ± 0.03	14
$^{19/18}$F-PSMA-1007	4.2 ± 0.5	118 ± 5	- 1.6 ± 0.02	98

9. Supplemental Data 2

Supplemental Table 2. Biodistribution of ^{68}Ga-^{19}F-rhPSMA-7 to 10, ^{18}F-rhPSMA-7 and the reference ligands ^{18}F-DCFPyL and ^{18}F-PSMA-1007 at 1 h p.i. in LNCaP tumor-bearing SCID mice (n=3 for ^{68}Ga-^{19}F-rhPSMA-7 to 9, n=3 for ^{18}F-rhPSMA-7, n=4 for ^{68}Ga-^{19}F-rhPSMA-10, ^{18}F-DCFPyL and ^{18}F-PSMA-1007). Data for reference ligands were taken from a previously published study by our group (*3*). Values are expressed as a percentage of injected dose per gram (%ID/g), mean ± standard deviation.

Organ	^{18}F-DCFPyL	^{18}F-PSMA-1007	^{68}Ga-^{nat}F-rhPSMA-7	^{68}Ga-^{nat}F-rhPSMA-8	^{68}Ga-^{nat}F-rhPSMA-9	^{68}Ga-^{nat}F-rhPSMA-10	^{18}F-rhPSMA-7 (uncomplexed)
Blood	0.34 ± 0.30	0.48 ± 0.29	1.9 ± 0.1	1.7 ± 0.1	0.46 ± 0.11	1.5 ± 0.3	1.9 ± 0.8
Heart	0.25 ± 0.09	1.4 ± 0.5	1.2 ± 0.3	0.93 ± 0.08	0.48 ± 0.17	0.75 ± 0.13	1.0 ± 0.4
Lung	0.46 ± 0.05	1.8 ± 1.0	1.7 ± 0.2	1.3 ± 0.2	0.94 ± 0.20	1.3 ± 0.2	2.0 ± 0.7
Liver	1.7 ± 0.2	1.2 ± 0.5	0.77 ± 0.10	0.79 ± 0.17	0.42 ± 0.07	0.70 ± 0.20	0.91 ± 0.21
Spleen	9.6 ± 4.4	16.68 ± 5.09	13.8 ± 5.0	6.3 ± 1.5	25.4 ± 5.2	9.4 ± 1.6	11.0 ± 2.9
Pancreas	0.20 ± 0.10	1.4 ± 0.7	0.71 ± 0.11	0.48 ± 0.11	0.39 ± 0.09	0.51 ± 0.03	0.55 ± 0.18
Stomach	0.20 ± 0.03	0.96 ± 0.86	0.51 ± 0.07	0.42 ± 0.11	0.48 ± 0.40	0.42 ± 0.12	0.66 ± 0.18
Intestine	0.14 ± 0.02	1.1 ± 0.3	0.43 ± 0.07	0.35 ± 0.01	0.44 ± 0.34	0.47 ± 0.21	0.67 ± 0.23
Kidneys	152.4 ± 15.3	123.3 ± 52.1	34.1 ± 6.6	82.3 ± 5.9	54.9 ± 3.0	77.5 ± 13.6	71.9 ± 6.8
Adrenals	5.0 ± 4.0	7.5 ± 3.4	6.7 ± 2.2	2.2 ± 0.8	2.7 ± 0.2	2.2 ± 0.3	14.6 ± 7.0
Muscle	0.11 ± 0.02	0.64 ± 0.41	0.42 ± 0.22	0.24 ± 0.02	0.19 ± 0.06	0.33 ± 0.10	0.37 ± 0.14
Bone	0.12 ± 0.02	0.89 ± 0.67	0.52 ± 0.11	0.32 ± 0.07	0.18 ± 0.05	0.35 ± 0.13	0.70 ± 0.14
Tumor	7.3 ± 1.5	7.4 ± 0.7	8.6 ± 0.2	6.5 ± 0.8	7.2 ± 0.6	11.7 ± 1.9	5.5 ± 0.6

10. Supplemental Data 3

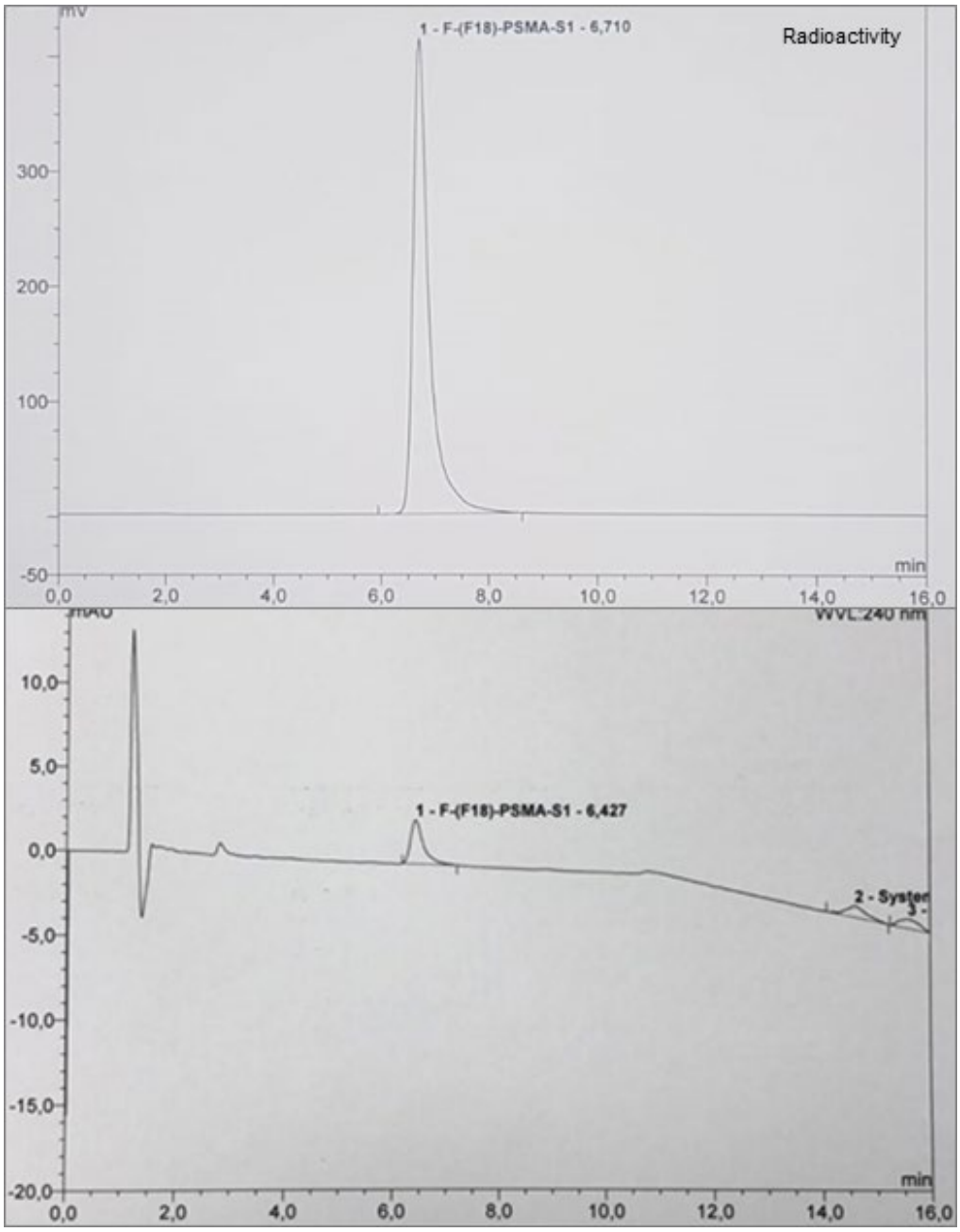

Supplemental Figure 13. Exemplary radio-HPLC analysis of ^{18}F-labelled rhPSMA-7 performed on a Prominence system, equipped with a variable wavelength detector (both Shimadzu) and a gamma-detector Gabi Star (Elysia-raytest, Straubenhardt, Germany). Water/0.1% TFA (solvent A) and MeCN/0.1% TFA (solvent B) served as mobile phases, a Nucleosil 100-5 C18 column of 125 × 4 mm was used as stationary phase. 10 µl of product solution were injected and the following linear solvent gradient was applied: 30-38

% B in 9 min, 38-95 % B in 8 min, back to 30% B in 1 min and re-equilibration at 30% B for 1.5 min (flow rate = 1 ml/min). Chemical impurities were monitored at 240 nm, the column temperature was set to 30 °C. The system was controlled by Chromeleon 6.8 Chromatography Data System Software (Thermo Fischer Scientific).

10. References

1. Weineisen M, Simecek J, Schottelius M, Schwaiger M, Wester HJ. Synthesis and preclinical evaluation of DOTAGA-conjugated PSMA ligands for functional imaging and endoradiotherapy of prostate cancer. *EJNMMI Res.* 2014;4:63.

2. Weineisen M, Schottelius M, Simecek J, et al. ^{68}Ga- and ^{177}Lu-Labeled PSMA I&T: Optimization of a PSMA-Targeted Theranostic Concept and First Proof-of-Concept Human Studies. *J Nucl Med.* 2015;56:1169-1176.

3. Robu S, Schmidt A, Eiber M, et al. Synthesis and preclinical evaluation of novel ^{18}F-labeled Glu-urea-Glu-based PSMA inhibitors for prostate cancer imaging: a comparison with ^{18}F-DCFPyl and ^{18}F-PSMA-1007. *EJNMMI Res.* 2018;8:30.

4. Iovkova L, Wängler B, Schirrmacher E, et al. para-Functionalized Aryl-di-tert-butylfluorosilanes as Potential Labeling Synthons for ^{18}F Radiopharmaceuticals. *Chem Eur J.* 2009;15:2140-2147.

5. Reich D, Wurzer A, Wirtz M, et al. Dendritic poly-chelator frameworks for multimeric bioconjugation. *Chem Commun.* 2017;53:2586-2589.

6. Notni J, Pohle K, Wester HJ. Comparative gallium-68 labeling of TRAP-, NOTA-, and DOTA-peptides: practical consequences for the future of gallium-68-PET. *EJNMMI Res.* 2012;2:28.

7. Valko K, Nunhuck S, Bevan C, Abraham MH, Reynolds DP. Fast gradient HPLC method to determine compounds binding to human serum albumin. Relationships with octanol/water and immobilized artificial membrane lipophilicity. *J Pharm Sci.* 2003;92:2236-2248.

8. Yamazaki K, Kanaoka M. Computational prediction of the plasma protein-binding percent of diverse pharmaceutical compounds. *J Pharm Sci.* 2004;93:1480-1494.